JOURNAL OF GEOPHYSICAL RESEARCH, VOL. 101, NO. D7, PAGES 12,639–12,657, MAY 20, 1996

Atmospheric deposition of reactive nitrogen oxides and ozone in a temperate deciduous forest and a subarctic woodland 1. Measurements and mechanisms

J. William Munger, Steven C. Wofsy, Peter S. Bakwin,[1] Song-Miao Fan,[2]
Michael L. Goulden, Bruce C. Daube, and Allen H. Goldstein[3]
Division of Applied Sciences and Department of Earth and Planetary Sciences, Harvard University, Cambridge, Massachusetts

Kathleen E. Moore, and David R. Fitzjarrald
Atmospheric Sciences Research Center, State University of New York at Albany

Abstract. We present 5 years of NO_y and O_3 eddy flux and concentration measurements and NO_x concentration measurements at Harvard Forest (1990-1994), a mixed deciduous forest in central Massachusetts, and 2 months of data for a spruce woodland near Schefferville, Quebec, during the NASA ABLE3B/Northern Wetlands Study (1990). Mean midday values of net dry NO_y flux from atmosphere to canopy were 3.4 and 3.2 μmole m^{-2} hr^{-1} at Harvard Forest in summer and winter, respectively, and 0.5 μmole m^{-2} hr^{-1} at Schefferville during summer. Nighttime values were 1.3, 2.0, and 0.15 μmole m^{-2} hr^{-1}, respectively. For 1990-1994, the net annual dry deposition of nitrogen oxides was 17.9 mmole m^{-2} yr^{-1} (2.49 kgN ha^{-1} y^{-1}). Oxidized species such as HNO_3 dominated N deposition, with minor contributions from direct deposition of NO_2. Emissions of NO from the forest soil were negligible compared to deposition. Comparison of NO_y deposition at Harvard Forest and Schefferville and analysis of the dependence on meteorological parameters show that anthropogenic sources dominate the nitrogen oxide inputs over much of North America. Heterogeneous reactions account for >90% of the conversion of NO_2 to HNO_3 in winter, leading to rates for dry deposition of NO_y similar to fluxes in summer despite 10-fold decrease in OH concentrations. In summer, formation of HNO_3 by heterogeneous reactions (mainly at night) could provide 25-45% of the NO_2 oxidation.

1. Introduction

Anthropogenic emissions of nitrogen oxide free radicals ($NO_x \equiv NO + NO_2 + NO_3$) from combustion supply 30-40% of global nitrogen oxide emissions and 85% of regional emissions in North America [*Logan*, 1983; *Davidson*, 1991; *Houghton et al.*, 1995]. The primary species emitted is NO. The NO_x radicals interchange in the atmosphere in a few minutes and are converted on longer timescales (from hours to several days) to higher oxides such as nitric acid (HNO_3) and peroxyacetylnitrate (PAN) and, ultimately, are removed from the atmosphere by precipitation and dry deposition. The family of nitrogen oxide species is collectively referred to as NO_y ($NO_y \equiv NO + NO_2 + NO_3 + N_2O_5 + HNO_3$ + PAN + other organonitrates + aerosol nitrate).

Deposition of nitrate supplies significant nutrient and acidity to ecosystems, and may potentially enhance rates of carbon storage [*Schindler and Bayley*, 1993]. Deposition of anthropogenic nitrogen has also been implicated as a stress factor in forest decline downwind of urban-industrial centers [*Schulze et al.*, 1989]. For example, *Aber et al.* [1989] have postulated that increased nitrogen inputs may lead to "nitrogen saturation," with long-term decline of soil fertility as cations are leached along with excess nitrate [*Durka et al.*, 1994]. Emissions of NO_x have a major impact on photochemical production and loss of O_3, which is also a stress factor for vegetation and human health [*Liu et al.*, 1987; *Chameides et al.*, 1994]. Concentrations of O_3 in turn affect rates of NO_x oxidation, making a coupled system that should be examined as a whole: to understand anthropogenic perturbations to NO_x, to O_3, and to nitrate deposition, it is necessary to determine the factors that control the export of nitrogen oxides from industrial source regions to the global environment, to define the rates for chemical transformation within the region, and to quantify the factors affecting deposition of nitrogen oxides to sensitive ecosystems.

Extensive measurements of reactive nitrogen concentrations during the summer season have been reported for the nonurban troposphere [see *Carroll and Thompson*, 1995, and references therein], but there are few year-round observations; there are very few flux determinations in any season.

This paper presents a 5-year data set of NO_y and O_3 eddy-covariance flux measurements at a deciduous forest in rural New England, along with simultaneous measurements of concentration profiles for O_3, NO_2, and NO. For comparison we examine similar measurements for a 10-week period at a subarctic spruce woodland in Quebec. We can examine the contributions of chemical reaction, storage in the canopy layer, and emissions of NO by

[1] Now at Climate Monitoring and Diagnostics Laboratory, National Oceanic and Atmospheric Administration, Boulder, Colorado.
[2] Now at Atmospheric and Oceanic Sciences Program, Princeton University, Princeton, New Jersey.
[3] Now at University of California, Berkeley, Berkeley, California

Copyright 1996 by the American Geophysical Union.

Paper number 96JD00230.
0148-0227/96/96JD-00230$09.00

soils to the NO_y flux. The objectives are to demonstrate that dry-deposition fluxes of NO_y can be measured reliably using the eddy-covariance method and to define the factors controlling NO_y deposition rates. A subsequent paper (J.W. Munger, Atmospheric Deposition of Reactive Nitrogen Oxides and Ozone in a Temperate Deciduous Forest and a Sub-arctic Taiga Woodland. 2. Seasonal and annual trends, to be submitted to *J. Geophys. Res.*, 1996, hereinafter referred to as M96) compares total NO_y deposition (wet plus dry) with regional NO_x emissions to estimate the fraction of NO_x emissions that are exported to remote regions.

The dominant processes expected to affect deposition fluxes and concentrations of reactive species in the forest are rates for atmospheric oxidation, transport from regional sources, rates for turbulent transport in the atmosphere, and characteristics of the vegetation cover (e.g., leaf area index (LAI) and stomatal conductance). These processes are examined using the surrogates in the data set (wind direction, insolation, temperature, canopy development, atmospheric stability, mixed-layer depth, and NO_x/NO_y ratio) by conditional averaging of 5 years of continuous data to define the response of NO_y deposition fluxes to natural variations of environmental parameters on diurnal, synoptic, and seasonal timescales. Then we examine the role of proximity to source region and vegetation cover by comparing results from Harvard Forest with those from Schefferville, a remote site 1200 km to the north. We also compare NO_y dry-deposition fluxes to dry-deposition fluxes of O_3, which have previously been extensively studied [*Padro*, 1993, and references therein], to elucidate the role of stomatal processes in controlling NO_y deposition.

2. Methods

2.1. Site Descriptions

The measurements at Harvard Forest are part of an interdisciplinary experiment begun in 1989 to provide a long-term record of trace-gas concentrations and surface exchange fluxes, along with supporting measurements of the physical environment, at a rural continental site. The work was initiated with establishment of the (NSF) Long-Term Ecological Research (LTER) site and the associated studies undertaken by participants in the National Institute for Global Environmental Change at Harvard Forest (sponsored by the U.S. Department of Energy). In addition to the nitrogen oxide and ozone data discussed here, measurements at Harvard Forest include net ecosystem exchange of CO_2 [*Wofsy et al.*, 1993; *Goulden et al.*, 1996a b], concentrations and fluxes of C_2-C_6 hydrocarbons [*Goldstein*, 1994; *Goldstein et al.* 1995], and energy and momentum exchanges [*Moore et al.*, 1996]. Complete data sets are available by anonymous ftp and World Wide Web.

Harvard Forest is located in Petersham, Massachusetts (42°32′ N, 72°11′ W), at an elevation of 340 m (Figure 1), 100 km west of Boston, Massachusetts, and 100 km northeast of Hartford, Connecticut. The surroundings are moderately hilly (relief ≈ 30 m), but there is no evidence of anomalous flow patterns that would make eddy-flux measurements at this site unrepresentative [*Moore et al.*, 1996], and the local energy budget is closed to within 15% [*Goulden et al.*, 1996b]. Within 200 km of Harvard Forest, regional NO_x emission densities range from 100 μmole $m^{-2}d^{-1}$ in the northwest (NW) sector to 650 μmole $m^{-2}d^{-1}$ in the southwest (SW) sector [*Environmental Protection Agency*, 1989].

The site is accessible by a dirt road closed to public traffic. The nearest secondary road passes ≈ 2 km to the west, and a main highway passes ≈ 5 km to the north. The forest at the site is 50 - 70 years old, predominantly red oak with red maple, scattered stands of hemlock and white pine, and plantations of red pine (located mostly to the southwest). The LAI is 3.4 for deciduous trees as determined by leaf collection. Measurements were made from a 30-m tower (Rohn 25G) extending 6 m above the average canopy height, erected in May 1989 with minimal disturbance of the vegetation. The instruments are housed in an air-conditioned shack 15 m east of the tower base.

The Arctic Boundary Layer Expedition (ABLE) 3B tower site was located 13 km NW of Schefferville, P.Q., Canada (54°50′ N, 66°40′W) at an elevation of 500 m [*Fitzjarrald and Moore*, 1994] during the summer of 1990. A lightly traveled gravel road ran 300 m to the west of the site. Besides Schefferville (population < 500) and a few smaller villages the nearest habitations are over 200 km to the south. The site was surrounded by an open black spruce woodland with extensive lichen groundcover and some shrubs. Average canopy height was 5-6 m. The measurements were made from a 30-m tower (Rohn 25G). The instruments were housed in a "weatherport" tent about 20 m SE of the tower base. Power was provided by a diesel generator located 300 m to the SE.

2.2. Eddy-Covariance Fluxes of NO_y

Determination of reactive nitrogen exchange across the canopy-atmosphere interface is problematic because multiple species with complex chemical interactions are involved, and unresolved analytical and micrometeorological issues remain. Reactive nitrogen fluxes across the canopy-atmosphere interface have been determined by indirect methods [*Geigert et al.*, 1994; *Johnson and Lindberg*, 1992; *Meyers et al.*, 1991; *Hanson and Lindberg*, 1991], profile methods [*Huebert and Robert*, 1985; *Lovett and Lindberg*, 1986; *Meyers et al.*, 1989; *Müller et al.*, 1993], and eddy covariance [*Hicks et al.*, 1989; *Stocker et al.*, 1993; *Wesely et al.*, 1982, 1983]. *Raupach et al.* [1991] demonstrated in the laboratory that there was a constant flux "roughness sublayer" for which the flux-gradient relationships over a plane surface with tall vegetation are different from those applicable over short canopies. *Fitzjarrald and Moore* [1994] and *Fazu and Schwerdfeger* [1989] found that this region can extend beyond three canopy heights. The existence of such difficulties argues for the use of the eddy-covariance technique within the constant flux layer in preference to profile methods.

The mass balance equation (neglecting horizontal advection) is given by

$$F_i^h + \frac{\partial}{\partial t}\int_0^h C_i(z)\,dz = \int_0^h P_i(z)\,dz - \int_0^h L_i(z)\,dz - \int_0^h D_i(z)\,dz, \quad (1)$$

where F_i^h is the turbulent flux of species i at a reference height h, $C_i(z)$ is the concentration (integrated over height to get the storage term), $P_i(z)$ and $L_i(z)$ represent the height-dependent chemical production and loss rates, respectively, and $D_i(z)$ is the height-dependent deposition to (or source from) surfaces. Equation (1) defines the terms that must be quantified in order to relate observed fluxes (first term on left) to a deposition (last term) in the layer. Examination of the NO-NO_2-O_3 system [*Fitzjarrald and Lenschow*, 1983; *Gao et al.*, 1991; *Kramm et al.*, 1991] indicates that fluxes of NO and NO_2 and, in some circumstances, O_3 may vary with height due to chemical reactions in the surface layer. It is extremely difficult to make separate determinations of the flux and concentration of each reactant or depositing species at multiple heights with sufficient accuracy to resolve these terms.

Alternatively, chemical species can be measured as groups of compounds that are conserved chemically on timescales relevant to turbulent exchange in a forest canopy. Chemical loss of NO_x via conversion of NO_2 to HNO_3 or formation of PAN has a char-

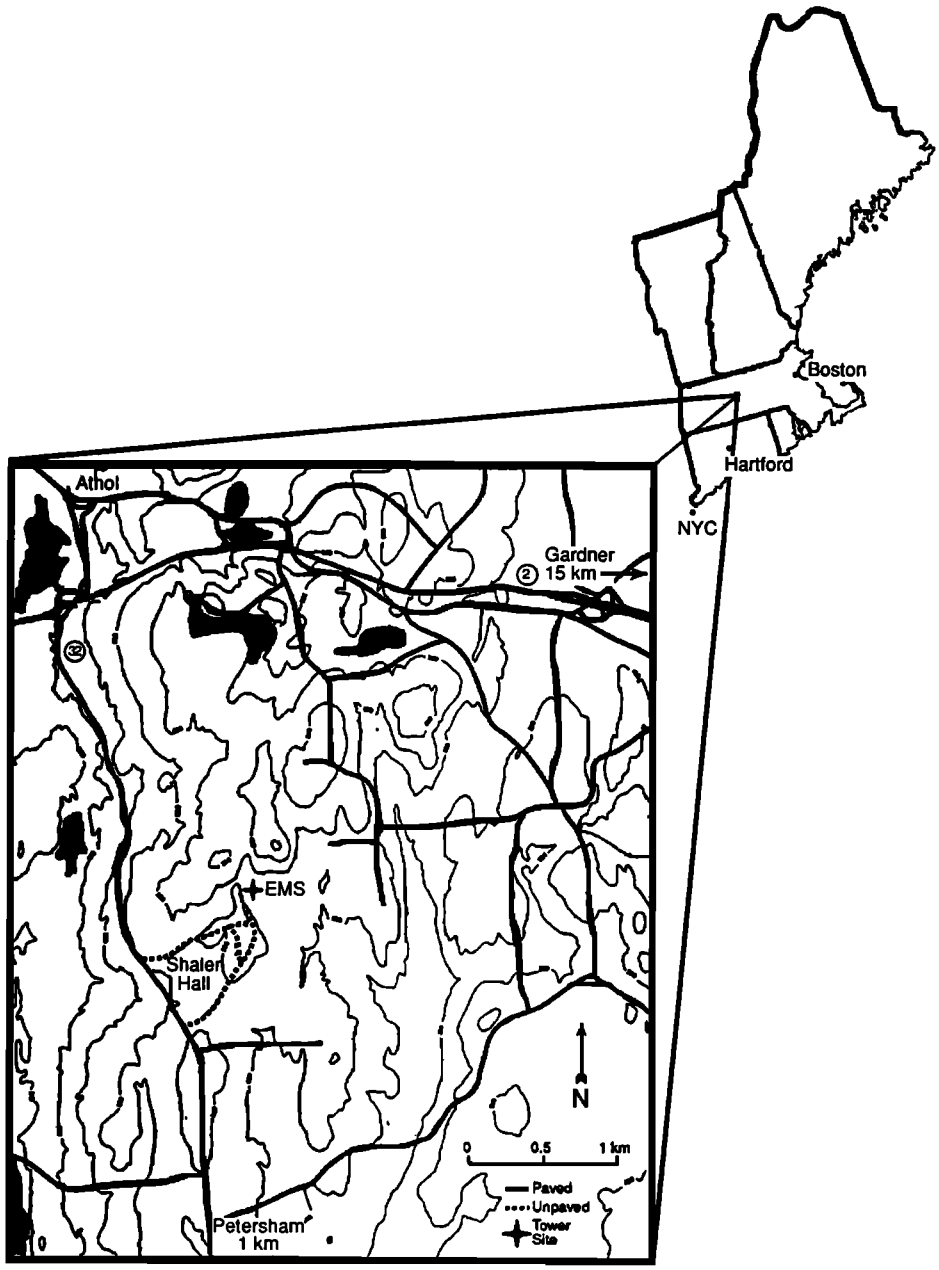

Figure 1. Map of immediate surroundings of Harvard Forest and its location relative to urban areas in the northeastern United States. The major highways and nearby towns are indicated. Contour intervals are 30 m.

acteristic time of several hours to a day for typical ambient concentrations, thus NO_x can be considered chemically inert. NO_y is not chemically produced or destroyed in the troposphere. Ozone is rapidly produced and consumed in the atmosphere as part of the NO-NO_2-O_3 photochemical cycle, posing a problem for measuring NO or NO_2 fluxes. However, in summertime at rural sites, O_3 concentrations are at least 10-fold greater than NO_x concentrations, and because local conditions are near photochemical equilibrium, the net photochemical change in O_3 is very small. For summertime mean conditions at Harvard Forest, we calculate a net O_3 production above the canopy, shifting to net O_3 loss in the shaded canopy, but the net reaction rates integrated through the canopy layer never exceed 20% of the observed O_3 flux; net rates were significantly less than that for most hours of the day. A more refined calculation of photochemical equilibrium would require inclusion of peroxy radicals. Note that the contribution of in situ reactions to the observed O_3 flux may be more important at sites with higher NO_x concentrations relative to O_3 or with large soil emissions of NO.

To correctly determine fluxes of chemical groups, it is absolutely essential that sensor response be constant for all components. For example, NO_x analyzers using photolytic conversion of NO_2 to NO do not have unit conversion efficiency; fluctuations in NO/NO_2 partitioning will be observed as a turbulent flux if changes in partitioning correlate with vertical wind. Likewise, even small interferences by compounds with vertical gradients may be unacceptable for eddy-flux measurements. Currently available NO_x sensors do not appear to be adequate for eddy-covariance flux measurements.

Suitable methods, however, are practical for NO_y but must be carefully applied. Although NO_y includes many species, which complicates interpretation of the NO_y flux, HNO_3 and NO_2

account for N deposition in most conditions. At sites with significant NH_3 emissions, formation of NH_4NO_3 aerosol [*Kramm and Dlugi,* 1994] may affect NO_y fluxes if particles are not quantitatively sampled. An efflux of NO from soils may contribute to NO_y flux, although it has been suggested that only a small fraction of this NO escapes from a forest canopy [*Bakwin et al.*, 1990]. By using additional data to constrain the magnitudes of individual component fluxes, the processes controlling reactive nitrogen exchange can be inferred from NO_y flux data. Furthermore, the measured NO_y flux can be directly interpreted as the net exchange of reactive N between the atmosphere and the ecosystem.

2.3. Measurement Methods

NO_y. Total nitrogen oxide, NO_y, was determined following reduction to NO by H_2 on a hot gold catalyst [*Bollinger et al.*, 1983; *Fahey et al.*, 1986] as described by *Bakwin et al.* [1994]. We preferred H_2 to the more commonly used CO due to lower toxicity and higher purity. The catalyst was located at the inlet to prevent adsorption of species such as HNO_3 to the tubing walls. NO was quantified by counting photon pulses from NO_2 chemiluminescence following reaction of NO with O_3 reaction [*Kley and McFarland*, 1980; *Ridley et al.*, 1987]. Air was sampled at a flow rate of ~900 $cm^3 min^{-1}$ (STP) through 15 m of 3 mm (OD) and 20 m of 6 mm (OD) Teflon tubing. Pressure in the detector cell (270 cm^3 total volume) was 13-20 mbar.

We estimate the fraction of aerosol nitrate aspirated by our inlet using experimental results for inlets at right angles to the wind [*Davies and Subari*, 1982]. Collection efficiency for particles varies inversely with the horizontal wind speed (u) raised to the power 1.5. For our sampling conditions the 50% cutoff diameter decreases from 14 to 2.5 μm for wind speeds 1-10 m s^{-1}. Measurements made at selected times throughout the year indicate that total aerosol nitrate at Harvard Forest was 16 - 40% of the nitrate + HNO_3 (B. Lefer and B. Talbot, unpublished data, 1995). Based on a limited number of measurements, we infer that the coarse aerosol (d > 2.5 μm), which the catalyst inlet partially excludes (at high wind speed), may contribute up to an additional 15% to dry deposition of NO_y at this site (H. Sievering, unpublished data, 1995).

The catalyst used at Schefferville and installed initially at Harvard Forest, was a 90 cm x 0.635 cm (ID) copper tube plated with gold (2.5 μm thick), in an "S" configuration [*Bakwin et al.*, 1994]. This configuration efficiently reduced NO_y to NO. However, after some time the underlying copper migrated to the surface and oxidized to CuO, which efficiently oxidized H_2, causing the sample line to freeze during cold weather. The catalyst at Harvard Forest was replaced in February 1991 with a 40.5 x 0.5 cm (ID) gold tube. Failures of the catalyst heater and vacuum pumps accounted for several data gaps during 1990 and 1991 (see section 3.2). Conversion to a perfluoro polyether pump oil (Fomblin) and a Reitschle model VCA-15-02 vacuum pump has virtually eliminated pump failures. Except for occasional gaps due to failures of the data acquisition and control system, preventive maintenance, or storm damage (seven lightning strikes and a downed power line at Harvard Forest so far), the NO_y system has operated nearly continuously from March 1991 to June 1995.

Background counts for the NO_y system were determined by adding a stream of O_3 in zero air, generated by a Hg-vapor lamp, to remove NO from the sample stream just downstream of the catalyst. The instrument response was determined by standard addition of NO in N_2 (Scott Specialty Gases, Plumbsteadville, Pennsylvania or Scott-Marrin, Riverside, California) at the inlet every 4 - 6 hours. Additions of HNO_3 were performed manually (see below). The NO standard was calibrated in the lab against archival standards from National Institute of Standards and Technology (NIST). Background count rates were typically 250 s^{-1}; the instrument response over the study period has been maintained in the range 0.25 - 0.75 part per trillion, volume (pptv = 10^{-12} cm^3 cm^{-3}) $count^{-1}$, depending on sample flow rates and ozonizer performance.

NO_x profiles. Concentration profiles of NO and NO_2 were determined above and through the canopy (29, 24.1, 18.3,12.7, 7.5, 4.5,0.8, and 0.3 m at Harvard Forest; 30.8, 18.2, 9.5, 6.2, 2.8, 0.85,and 0.05 m at Schefferville) using a separate chemiluminescence NO detector with a Xe-lamp photolysis cell (60 cm^3) to convert NO_2 to NO [*Bakwin et al.*, 1992] (until August of 1990 the NO/NO_2 sensor at Harvard Forest sampled only from the 30-m level). The profile inlets were sequentially sampled by operating Teflon solenoid valves mounted at a central Teflon hub on the tower and flushed by an excess flow through a bypass pump. The profile line (4 mm ID Teflon) was maintained at a reduced pressure (590 mbar) to prevent condensation. Sampling inlets nearest the ground (< 5 m) were located away from the disturbed area near the tower base. Failures of the vacuum pump and Xe lamp and other breakdowns led to significant data gaps for one or the other NO_x component at Harvard Forest (see section 3.2).

The NO/NO_2 system was calibrated by standard addition of NO in N_2 to the sample stream immediately behind the central hub, located 15 m above the ground on the tower. The NO_2 photolysis efficiency was determined by adding NO_2 from a permeation tube (or NO_2 in N_2 after November 1993) to the sample. The NO_2 source was calibrated against the NO standard, and NO_2 artifacts in the photolysis cell were determined, by periodically placing a hot-gold catalyst immediately upstream of the NO_x detector to quantitatively convert NO_2 to NO. Artifact NO_2 (< 50 pptv) was associated with accumulated contamination in the photolysis cell and was periodically removed by rinsing with distilled H_2O. Variations in the permeation rate over time were derived by linear interpolation between successive calibrations; periodic checks indicate the NO_2 cylinder has been stable.

The response of the NO_x detector to atmospheric NO is affected by ambient O_3 concentrations because of the reaction $NO + O_3 \rightarrow NO_2 + O_2$ in the tubing. The instrument response factor and its dependence on ambient O_3 was determined from standard additions several times a day over the course of each data collection interval (1-3 days). The apparent reaction rate between NO and O_3 in the tubing was about twice the expected gas-phase rate, consistent with previous observations [*Ridley et al.*, 1988; *Bakwin et al.*, 1992]. Corrections were made for differences in ambient O_3 between calibrations and at different sampling heights using the apparent reaction rate in the tubing determined from calibration data. The background signal (typically <160 count s^{-1}) for the NO_x detector was determined by adding O_3 in zero air from a Hg-vapor lamp upstream of the photolysis cell, analogous to the determination of the null signal for the NO_y detector.

O_3 measurements. We measured the vertical profiles of O_3 concentration by UV absorbance (Dasibi 1003AH). The concentration of O_3 at 30 m was measured using C_2H_4-chemiluminescence instruments (at various times from Monitor Labs, Columbia Scientific, Bendix). The profile inlets were shared by O_3 and NO_x sensors. The eddy inlet for O_3 was a separate 4 mm ID Teflon tube, flushed by excess flow through a bypass pump to reduce transit time. Calibration of the Dasibi was checked periodically by comparison to a calibration unit (Dasibi 1008PC), or by returning the instrument to the factory. The calibration of the C_2H_4-chemiluminescence instrument was checked during each profile by comparison to the Dasibi measurement at 29 m.

Precision and accuracy. The overall accuracy of the NO_x and NO_y measurements was estimated to be ± 6%, mainly from uncertainty in flowmeter calibrations and in the concentration of the calibration standards obtained from NIST. The analytical precision was estimated to be ≈4% from the coefficient of variation (CV) of NO_y calibration factors over 2-month periods. Reported concentrations are based on average calibration factors over 3-day intervals; the CV at this scale is 2.5% for NO_y. The precision of the NO measurements was ≈4%, estimated by computing the CV of the residual from a least-squares fit of the NO gain versus ambient O_3 concentration. The CV of the NO_2 photolysis efficiency, after removing linear trends due to aging of the photolysis lamps, was 7%. The minimum detection limit for NO, NO_2 or NO_y, estimated from twice the 1-min standard deviation during a zero check, was ≈ 50 pptv at Harvard Forest and < 10 pptv at Schefferville (the NO_x and NO_y detectors at Schefferville were optimized for maximum sensitivity, whereas the Harvard Forest instruments had reduced sensitivity to prevent the 16-bit photon counter from wrapping and to minimize counter coincidence errors during pollution episodes). Corrections for counter coincidence were less than 5% for counting rates below 10^5 s^{-1} (≈ 25 parts per billion, volume (ppbv = 10^{-9} cm^3 cm^{-3}), typically). The detection limits and sensitivity were only an issue for the NO results (at both sites) and for vertical gradients of NO_2 (at Schefferville); observed concentrations of NO_y and NO_2 at Harvard Forest were always well above detection limits.

Eddy covariance fluxes. Vertical and horizontal wind velocities and virtual temperature (calculated from the speed of sound) at 30 m were determined at Harvard Forest using a three-axis sonic anemometer (Applied Technologies, SWS-211/3K) mounted on a boom oriented toward the west, so the transducer array faced into prevailing winds. At Schefferville the sonic anemometer was rotated to face the wind [*Fitzjarrald and Moore*, 1994]. The eddy O_3 inlet was suspended from the anemometer boom (at Harvard Forest) or from a separate boom (Schefferville). The NO_y catalyst inlet was located on a separate boom 0.73 m below and behind the sonic anemometer because it has significant cross section (5x40 cm) and is a source of heat.

Outputs from the fast-response sensors used for flux computations were recorded at 4 Hz (8 Hz for NO_x and NO_y), and the remaining sensors were recorded at 0.5 Hz. Data were stored on a PC-based data acquisition and control system and downloaded every 2-3 days.

Fluxes were calculated for 30-min intervals from the covariance of vertical wind velocity (w') with fluctuations of temperature (T') or trace-gas concentrations (C'), after removing a linear trend [*Fan et al.*, 1990, 1992]. To minimize phase shifts between concentrations and the vertical wind, w' was numerically filtered using a low-pass filter having a time constant appropriate for each sensor before computing the covariances; the time constant was determined for each sensor system from the observed response to a standard addition near the inlet (see section 3.1). In the flux computation, raw data from closed-path sensors were offset by the observed time lag to account for transit time in the tubing. Lag times were computed from the maximum covariances of w' and C' in a lagged covariance plot (see section 3.1) in good agreement with measured transit times for the standard additions. To estimate the flux potentially lost by attenuation of concentration fluctuations in the tubing and detector cells [*Lenschow and Raupach*, 1991; *Massman*, 1991], we applied a numerical low-pass filter to w' and T' as appropriate for the NO_y sensor, computed the heat flux, and compared it to the heat flux computed from raw data. Tracer fluxes were corrected (10-20%) by the ratio of raw to filtered heat fluxes for each 30-min interval. Small errors in leveling the sonic anemometer or deviations from horizontal streamlines were corrected by axis rotation in the flux-calculation routines [*McMillen*, 1988]. Corrections for changes in density [*Webb et al.*, 1980] were not necessary for NO_y and O_3 fluxes. Pressure and temperature were held constant by the instruments and the remaining correction term for water vapor fluctuations was negligible.

3. Results

3.1. Method Validation

In addition to the customary constraint of no horizontal advection and the need to eliminate or account for storage and chemical reaction terms that are included in equation (1), accurate NO_y flux measurements by eddy covariance require from the sensor that (1) there be minimal loss of NO_y species at the sampling inlet (2) all NO_y species be converted to NO rapidly and efficiently by the catalyst and (3) fluctuations in concentration pass without attenuation by dispersion during transit from inlet to sensor. Elimination of any sample inlet upstream of the catalyst avoided NO_y retention. Routine checks of NO_2 conversion efficiency show no significant changes of catalyst performance with time. Evaluation of step concentration changes from adding NO calibration standard at the inlet (Figure 2a) indicates an overall response time for the instrument that is approximated by an exponential decay with a 1-s time constant, for a sample flow rate of ~ 900 $cm^3 min^{-1}$ (mass flow at STP). The Reynolds number (*Re*) for this flow is less than 760, leading to laminar flow throughout the sample tube. Although turbulent flow is the ideal situation for eddy-covariance measurements [*Lenschow and Raupach*, 1991; *Massman*, 1991], as we will see below, the fluctuations associated with turbulent fluxes to the forest canopy were predominantly at lower frequencies and not significantly attenuated. Increasing sample flow to reduce the response time and induce turbulent flow would reduce the catalyst efficiency and sensitivity of the NO detector. For comparison, a parallel CO_2 instrument and calibration system with a flow ~ 7000 $cm^3 min^{-1}$ (*Re*= 2400) exhibits an exponential time constant, $\tau = 0.25$ s.

We measured the response of the system to pulses of HNO_3 introduced at the inlet (Figure 2b). There was slight retention of HNO_3 compared to NO_2. The signal decay fits a double exponential, with small (<10%) amplitude for the slow component. The present catalyst design eliminates nearly all surfaces other than hot gold (short pieces of 1.6 mm OD stainless steel tubing are inserted at the inlet to deliver H_2 and calibration standard), minimizing wall adsorption and signal dispersion [cf. *Bakwin et al.*, 1992].

The peak in the $\langle w'NO_y' \rangle$ lagged correlation plot shows an unavoidably long (27 s) delay for transit through the tubing, but there was no indication of significant peak broadening or asymmetry compared to the $\langle w'T' \rangle$ covariance (Figure 3a). To simulate the influence of attenuation, we apply low-pass filtering to the $\langle w'T' \rangle$ covariance using a 1-s exponential time constant. Attenuation (dashed line) has a negligible effect on the shape of $\langle w'T' \rangle$ covariance peak for the example shown. Evaluation of cospectra (Figure 3) indicate that most of the flux is carried by eddies in the 0.005 to 0.5-Hz range (horizontal extent = 2 - 200 m for a 1 ms^{-1} wind). For the period illustrated there is minimal loss of $\langle w'NO_y' \rangle$ covariance at high frequencies compared to $\langle w'T' \rangle$, though on average, the correction for attenuation of high-frequency components of the flux was 10-17%, with generally smaller corrections during the daytime when large-scale turbulence dominated.

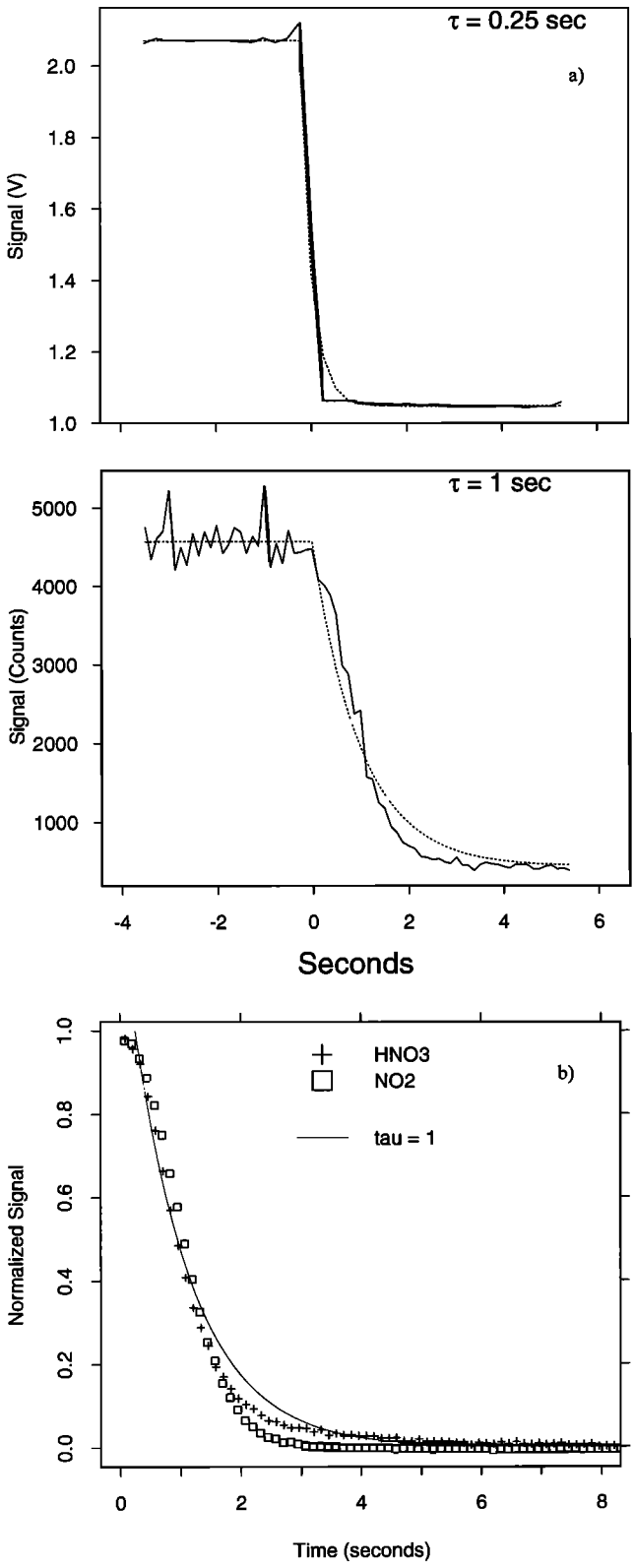

Figure 2. (a). Instrument responses to a step change in CO_2 (top panel) and NO (bottom panel) gas flow at the inlet are shown by solid lines. The dashed lines correspond to exponential decay curves with $\tau = 0.25$ s for CO_2 and $\tau = 1$ s for NO. The data for CO_2 signal were recorded at 4 Hz; NO_y counts are recorded at 8 Hz. (b). Normalized signal for a puff of HNO_3 (pluses) or NO_2 (squares) dispersed at the NO_y inlet under field conditions. The data points are individual 8-Hz photon counts normalized by the difference between initial and final signals $((C(i) - C_\infty)/(C_0 - C_\infty))$. The line indicates an exponential decay with $\tau = 1$ s.

3.2. Hourly and Daily Data

Examples of time-series data for short intervals. Hourly observations for the period September 8-13, 1992 (Figure 4), illustrate diurnal and synoptic variations typical of observations at Harvard Forest. Elevated concentrations of NO_y and moderate O_3 levels, associated with temperatures > 20°C and southwesterly winds, were observed on September 8 and 9. NO_x/NO_y ratios varied from < 0.5 to ~1. Ozone concentrations showed afternoon maxima throughout the period. Variations of NO_x and NO_y concentrations were less systematic, with a tendency for higher concentrations at night. A sharp drop in temperature and a shift to northerly winds, following passage of a cold front on September 10, brought markedly lower NO_y and O_3 concentrations. Peak NO_y eddy fluxes coincided with peaks in the quantity NO_y - NO_x during the polluted period, indicating high concentrations of rapidly depositing species (e.g., HNO_3). Maximum O_3 fluxes coincided with peak photosynthetically-active photon flux density (PPFD). Fluxes of both NO_y and O_3 were negligible when vertical mixing in the surface layer was weak, as indicated by friction velocity ($u^* = \sqrt{\overline{w'u'}}$) < 0.1 ms^{-1}, for example, during the night of September 12. Low fluxes of NO_y were also observed during some turbulent nights, $u^* > 0.1$ m s^{-1}.

Hourly data for August 7-12, 1990, at Schefferville (Figure 4) illustrate a typical synoptic pattern of warming temperatures and increasing NO_y associated with advection of polluted air from industrial regions or forest fires in advance of an approaching low-pressure system. Concentrations and temperature dropped sharply as the front passed [*Bakwin et al.*, 1994]. Eddy fluxes of NO_y and O_3 at Schefferville usually followed consistent diel trends, with midday maxima. The fluxes were nearly zero on calm nights ($u^* < 0.1$ m s^{-1}) but remained steady on windy nights.

Examples of time-series data for 1991-1994. The time series of hourly mean NO_x, NO_y, and O_3 concentrations at Harvard Forest for 1991 - 1994 showed substantial diel and day-to-day variability (Figure 5a, top three panels). Severe pollution episodes were usually brief, lasting no more than a few hours. Concentrations of NO_x and NO_y maximized in winter and the frequency of concentrations > 30 ppbv increased. Concentrations of O_3 were highest in summer; peak hourly concentrations approached 80 ppbv and exceeded 100 ppbv a few days each year. Complete removal of O_3 (due to titration by NO) was observed regularly during winter. The time series of concentration data for Schefferville is shown by *Bakwin et al.* [1994]; corresponding NO_y and O_3 fluxes are shown in Figure 5b (O_3 concentrations reported here are slightly lower (10%) than those reported by *Bakwin et al.* [1994] due to a reevaluation of the instrument calibration data). Episodes of high NO_y concentration (> 1 ppbv) at Schefferville were due to transport from distant urban areas or forest fires.

Subcanopy storage. The shifts in concentrations that are evident in Figure 4 and Figure 5a have a random component due to synoptic events such as frontal passage and a systematic component due to mean diel concentration trends. The canopy storage term (equation (1)) determined from concentration profiles can be used to quantify the influence of systematic patterns, but the contribution from random shifts in concentration cannot by assessed because large vertical and horizontal heterogeneity in the concentration fields surrounding the tower makes individual hourly determinations of the canopy storage term highly variable. The effect of the canopy storage term associated with synoptic concentration shifts will be minimized, however, when averaging the flux data over long intervals as we will do here.

On average, O_3 concentrations within the canopy increase with time for a few hours after sunrise during summer at Harvard Forest. The measured flux therefore represents a slight (< 20%)

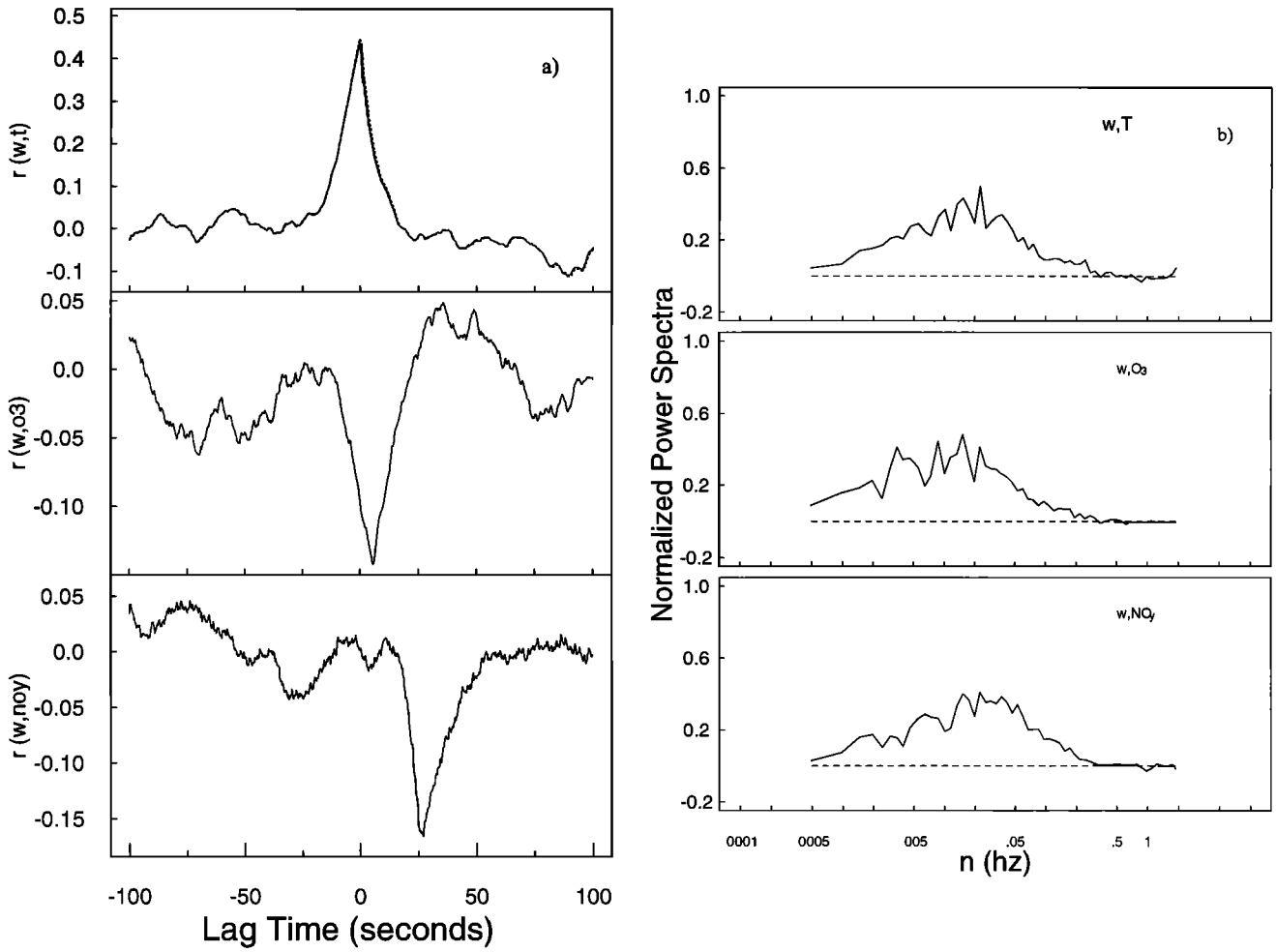

Figure 3. (a) Covariance of vertical wind speed with temperature (top panel), O_3 (middle panel) and NO_y (bottom panel) versus time offset. The covariance peak occurs at the lag time corresponding to transit time for air in the sample lines. The data shown are from 1300 (EST), September 13, 1992. (b) Normalized cospectra of T (top panel), O_3 (middle panel), and NO_y (bottom panel) with vertical wind are shown versus frequency. The plots are averages of cospectra computed each afternoon for 9 days, September 7-15, 1992.

overestimate of O_3 deposition; there is a corresponding underestimate of deposition in the early evening as O_3 concentrations decline (Figure 6a). During the afternoon when O_3 fluxes were at their peak, changes in O_3 storage were insignificant. Lower concentrations and weaker diel cycles reduce the importance of O_3 storage at Schefferville and at Harvard Forest in winter.

Vertical profiles were measured for NO_x but not for NO_y, so we cannot determine the total NO_y storage term. However, at Harvard Forest in summertime, changes in NO_x accounted for much of the diel trend in NO_y. Except for brief periods in early morning when canopy ventilation reduced NO_x concentrations and in the evening when NO_x concentrations increased, changes in NO_x storage were insignificant compared to the deposition at Harvard Forest in the summer (Figure 6b). Variations in NO_x concentrations were larger in winter, but changes in storage were not consistently different from 0; variability in the NO_x storage contributes to noise in the mean diel patterns for NO_y.

Because changes in storage are small relative to the mean fluxes and inclusion of the storage terms on an hourly basis would not reduce variability in the flux data, we do not correct the fluxes for canopy storage. Furthermore, changes in storage sum to zero over the course of a day and have no influence on cumulative daily fluxes.

Seasonal trends in concentrations and fluxes. The tendency toward higher NO_x and NO_y and lower O_3 concentrations during winter at Harvard Forest may be quantified using probability distributions for hourly means during midday (1000 - 1700 EST) as shown in Figure 7. Concentrations of NO_x and NO_y in winter were more than double summertime values for most fractiles. Note, however, that background concentrations of NO_y (as reflected by the 10 percentile) were constant from summer to winter, even though background concentrations of NO_x increased. The seasonal invariance of background NO_y concentrations at Harvard Forest suggests that atmospheric removal processes relative to emissions have similar efficiencies in summer and winter (see M96). The proximity to emission sources accounts for more frequent observations of high concentrations and the wider concentration range at Harvard Forest than at Schefferville.

The integrated daily dry-deposition fluxes of NO_y at Harvard Forest showed considerable day-to-day variability but did not shift systematically with season (Figure 5a, panel 4). This is a surprising observation: there is a significant seasonal cycle of NO_y concentrations (Figure 5a, panel 2), but it is not associated with corresponding variations in NO_y dry-deposition fluxes. In contrast, the fluxes of O_3 (Figure 5a, bottom panel) followed a clear seasonal trend with maxima during the growing seasons

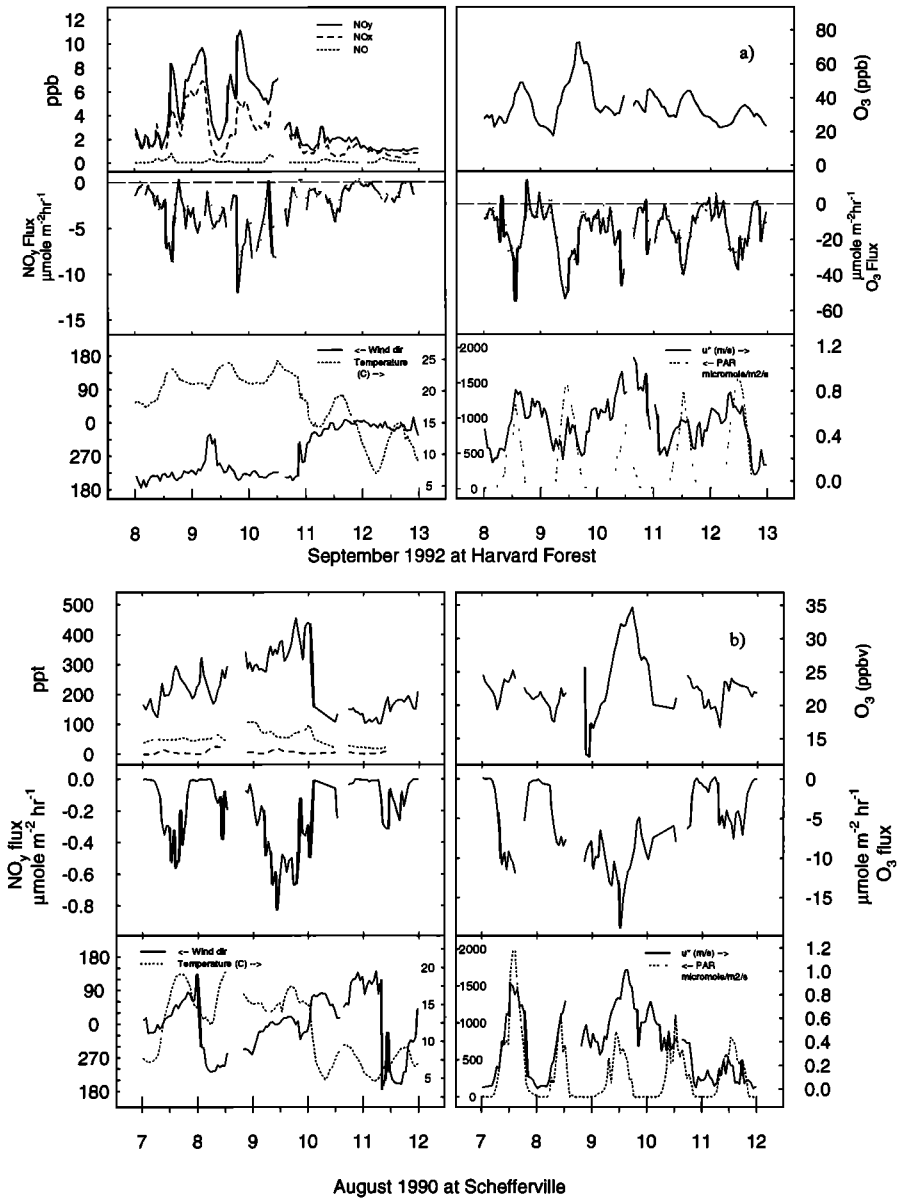

Figure 4. (a) Hourly averaged concentrations, fluxes, and selected meteorological parameters at Harvard Forest are shown for the period September 8-13, 1992. NO_y concentrations (solid line) are hourly means from continuous data; NO and NO_2 (short- and long-dashed lines, respectively) concentrations are given for the sample inlet at 30 m and represent ≈ two observations per hour. The 30-min integrated NO_y and O_3 fluxes without correction for loss of high frequencies are show as points; the lines show the hourly average flux after corrections are applied. Photosynthetically-active photon flux density (PPFD) values at noon under clear skies are ≈ 1500 µmole $m^{-2}s^{-1}$ in September. Times are given in eastern standard time. (b) Same as Figure 4a, but for August 7 - 12 at Schefferville.

each year, coincident with peak concentrations and with canopy development. These observations are discussed in detail below.

Dry deposition of NO_y exceeded 350 µmole m^{-2} d^{-1} on four days in the summer of 1990 (not shown in Figure 5 but included in overall statistics), but values never exceeded 300 µmole $m^{-2}d^{-1}$ in subsequent years. Diagnostic checks of flux data give no reason to invalidate the large fluxes in 1990. These data may reflect unusual atmospheric patterns or pollutant emissions that occur infrequently, but it is difficult to completely rule out an artifact in the data for 1990 associated with formation of CuO in the original catalyst. Conclusions derived from the 5-year time series are not significantly affected by the high values in 1990.

In general, the integrated daily NO_y fluxes at Schefferville (Figure 5b, top panel) (5-10 µmole m^{-2} d^{-1}) were less than 20% of the typical values at Harvard Forest. A substantial fraction of the NO_y dry deposition came during a few high-flux events that deposited more than 15 µmole m^{-2} d^{-1}. The integrated daily O_3 fluxes were less variable (Figure 5b, bottom panel), with a gradual decline in magnitude of daily total deposition over the summer following the decrease in day length (i.e., the period for stomatal activity and convective mixing).

4. Discussion

4.1. Diel and Seasonal Cycles of Concentrations

We focus here on comparison of summer (June, July, August) and winter (December, January, February) periods at Harvard Forest to elucidate seasonal changes. Data are segregated by

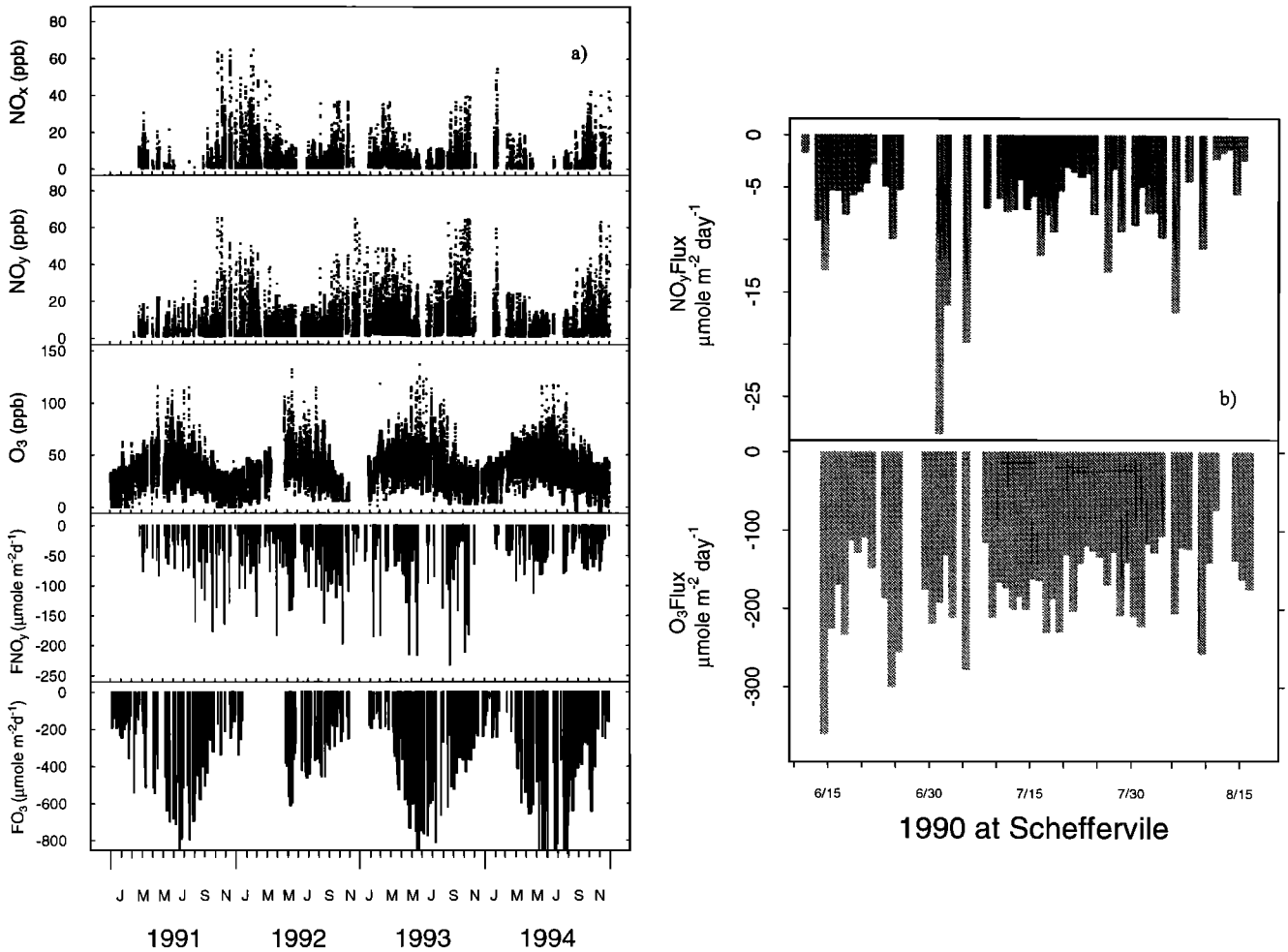

Figure 5. (a) Hourly average concentrations of NO_x, NO_y, and O_3 and daily integrated fluxes of NO_y and O_3 are shown for the period January 1991 to December 1994. The data for 1990, which have more gaps, are not shown. The plot of O_3 concentrations includes results from the profile instrument to fill in periods when the eddy instrument was not working. Instrument problems described in section 2.3 led to frequent gaps early in the sequence. Data recovery improved considerably over the course of the measurements. Fluxes on days with less than 4 missing hours were computed by interpolating between adjacent valid observations. Days with longer gaps were rejected. (b) Integrated daily fluxes of NO_y and O_3 are shown for the ABLE 3b campaign at Schefferville during summer 1990.

surface wind direction to contrast the clean NW sector (270°-45°) and polluted SW sector (180° - 270°). Analysis of back trajectories (J. Moody, University of Virginia, personal communication, 1995) identifies similar polluted and clean sectors. Spring and fall periods generally exhibited a blend of summer and winter patterns.

Diel trends in concentrations of NO_x, NO_y, O_3, and the NO_x/NO_y ratio are shown for summer and winter in Figure 8. The difference in emission density between the heavily urbanized SW sector and the rural NW sector accounted for distinct differences (factors of 2-3) in mean concentrations associated with NW and SW winds (Table 1). Easterly winds, which are relatively rare at Harvard Forest (omitted from figures for clarity), were associated with more variable concentrations showing both the influence of cities in eastern Massachusetts and Rhode Island and the occasional influx of relatively clean marine air. At Schefferville, mean NO_x and NO_y concentrations were lower than the summertime clean-sector means at Harvard Forest by about a factor of 10; the difference was larger for NO_x than for NO_y (see also Figure 7).

The diel changes in NO_x and NO_y concentrations had opposite phase at Harvard Forest compared to Schefferville (see Figure 8). This contrast is associated with differences in the vertical concentration gradients. The northeastern United States is a net NO_x emission region, hence on average, NO_x and NO_y concentrations decrease with height through the mixed layer [*Trainer et al.*, 1991; M. Trainer, unpublished data, 1993, over Harvard Forest]. Concentrations increase at night as surface emissions are trapped beneath a stable inversion layer. During the daytime, vertical mixing redistributes NO_x and NO_y through the planetary boundary layer, giving midday minima. Schefferville, however, is distant from most sources of NO_x and NO_y (except for sporadic forest fires). Concentrations near the surface are depleted by chemical reaction and deposition and replenished by downward mixing of elevated concentrations from the top of the boundary layer [*Sandholm et al.*, 1994; *Singh et al.*, 1994] during the day. Hence at Schefferville, concentrations of NO_x and NO_y had maxima during the daytime when vertical mixing was strongest (Figure 8, column 3).

The amplitude of the diel cycle at Harvard Forest was greatest during polluted conditions (SW wind sector) because of higher emission densities. The diel cycle for NW sector winds had a smaller amplitude because lower emission densities to the north-

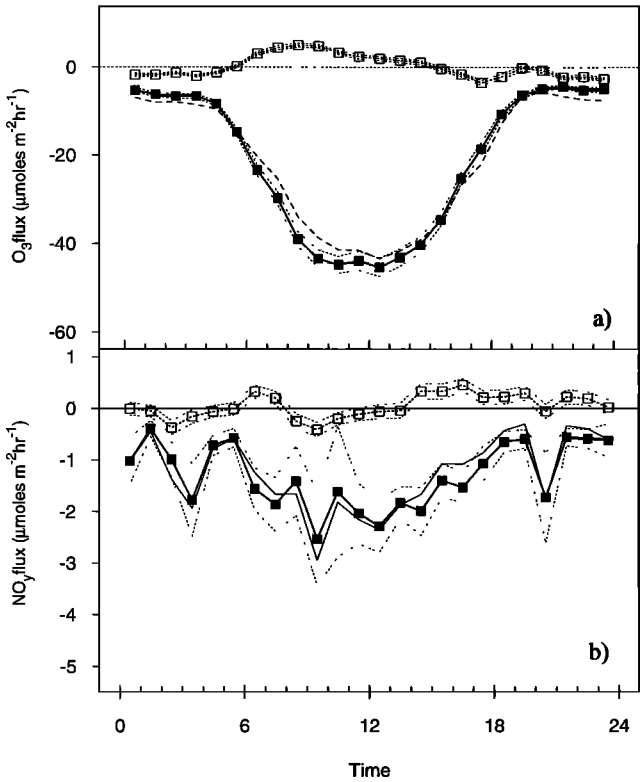

Figure 6. (a) Mean diel cycle of observed O_3 flux (solid squares) and storage term (open squares) computed for summer periods (June-August). Dashed lines indicate the standard errors about the mean. The integrated surface deposition (sum of flux and storage) is given by the solid line. (b) Mean diel cycle of observed NO_y flux (solid squares) and NO_x storage term (open squares) computed for summer periods. Dashed lines indicate the standard errors about the mean. The integrated surface deposition (sum of flux and storage) is given by the solid line.

west and better mixing associated with NW winds, which tend to occur following cold fronts, both reduce vertical gradients. In winter the boundary layer is shallow and convective mixing is weak, and day/night differences in concentration are relatively smaller than in summer. The shallow boundary layer during winter (about half the summertime depth) [*Holzworth*, 1967] partially accounts for the increase in mean concentrations of NO_y and NO_x at Harvard Forest from summer to winter. Concentrations of NO_x increase more than NO_y, reflecting slower rates for photochemical oxidation in winter.

At both Harvard Forest and Schefferville the diel variation of O_3 concentrations showed midday maxima, reflecting entrainment of elevated O_3 from aloft and the influence of photochemical reactions, as observed by *Kleinman et al.* [1994]. In winter, polluted air from the SW at Harvard Forest was depleted in O_3 due to titration by NO, whereas during summer, photochemical pollution contributed to 50% higher mean daytime O_3 compared to the NW sector. Concentrations of ozone at Schefferville were 10-20 ppbv (20 - 40%) lower than during clean periods at Harvard Forest.

The concentration ratio NO_x/NO_y (Figure 8, row 3) reflects the relative rates of NO_x emission, oxidation, and deposition of nonradicals such as HNO_3. Emission and deposition both increase the NO_x/NO_y ratio by adding fresh NO_x and depleting stable depositing species, respectively, whereas oxidation decreases this ratio by depleting NO_x. During winter the boundary layer at Harvard Forest is more strongly influenced by fresh NO_x emissions for periods with SW winds, accounting for significantly higher NO_x/NO_y compared to the NW. The ratios for both sectors were nearly independent of time of day, indicating that characteristic time for NO_x oxidation in winter exceeded a day and that the NO_x/NO_y ratio did not vary significantly with height within the boundary layer. In contrast, during summer, photochemical oxidation led to seasonally lower mean ratios for NO_x/NO_y, and there was a distinct diel cycle. During summer the NO_x/NO_y ratio dropped from ~ 0.5 at night, when fresh emissions accumulated in the surface layer, to near 0.2 during the day for both SW and NW wind sectors. The minimum NO_x/NO_y ratio occurred near noon when winds were from the NW sector, corresponding to peak insolation; the minimum occurred about two hours later, coincident with the peak in mean O_3, when winds were from the SW sector.

We observed simultaneous increases in NO_x, NO_y, and NO_x/NO_y and increases in O_3 during summer as boundary layer growth entrained aged pollutants after sunrise [*Kleinman et al.*, 1994].

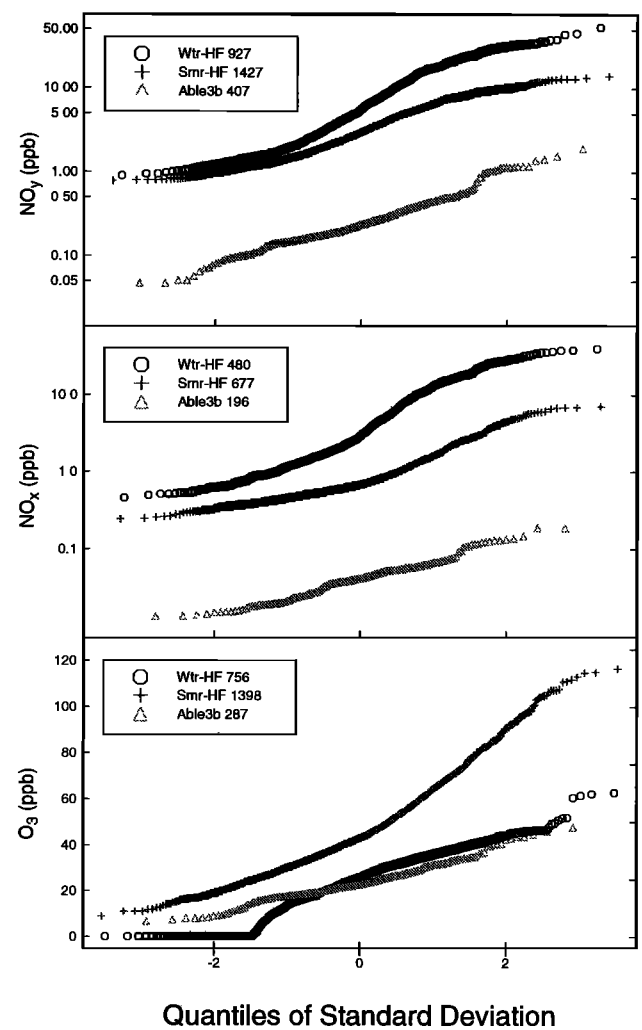

Figure 7. Cumulative probability plots of NO_y, NO_x, and O_3 concentrations (as quantiles of the standard normal distribution) for summer and winter at Harvard Forest and for July-August 1990 at Schefferville. The upper 5% and minimum 2.5% of the Harvard Forest data have been rejected to avoid skewing the distribution by observations that are unrepresentative of typical conditions. The number of observations for each category are given in the symbol legend.

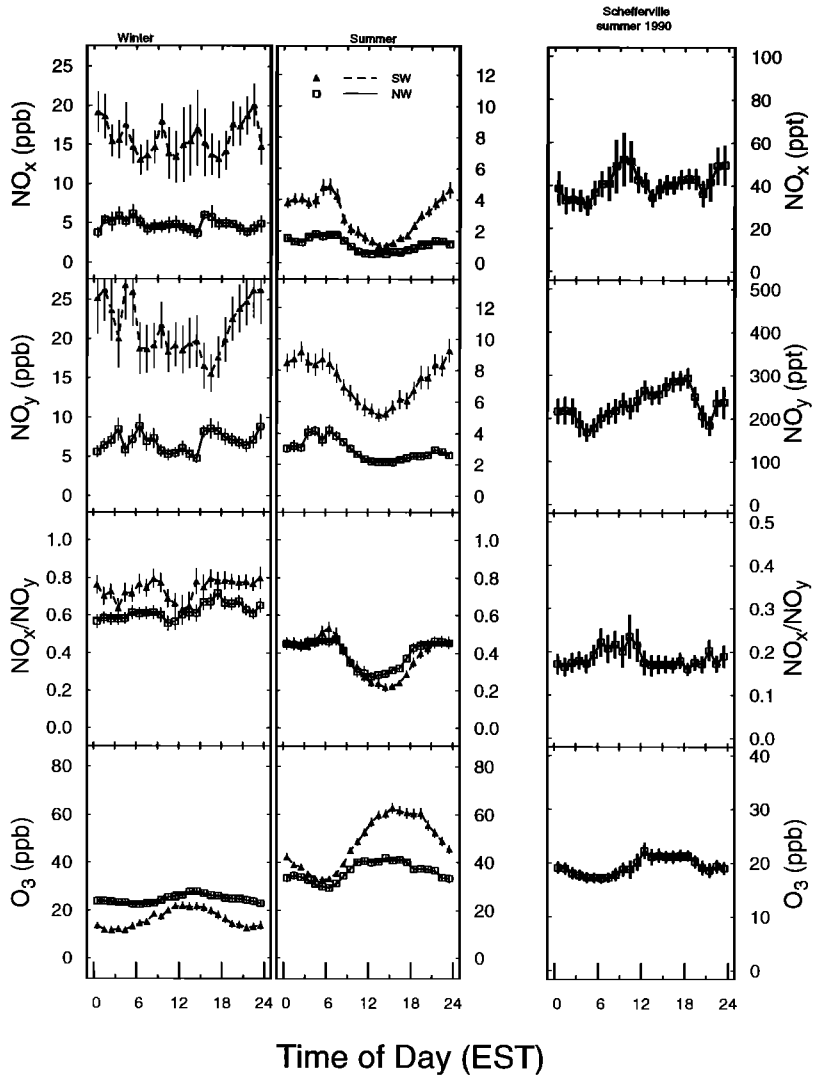

Figure 8. Mean diel cycles of NO_y, NO_x, NO_y/NO_x, and O_3 for winter (December - February) at Harvard Forest, column 1, and summer (June - August) at Harvard Forest, column 2, are shown for two dominant wind sectors: 270° - 45° (clean sector) is solid line and open square; 180° - 270° (polluted sector) is long-dashed line and solid triangle. Data for the period March 1990 - December 1994 are used. Vertical bars indicate the standard error about the mean. Very stable or unusually stormy periods are rejected by using only data for $0.1 < u^* < 1.5$ and $0.1 < u^* < 1$ m s^{-1} for winter and summer, respectively. Note the change of scale for NO_x and NO_y concentrations at Harvard Forest between winter and summer. Mean diel cycles ± standard error. for Schefferville are shown for the same conditions of $u^*(0.1 < u^* < 1$ m $s^{-1})$ in column 3. Note the change in scale.

Fresh emissions of NO_x were trapped near the surface during late afternoon and evening as rates for vertical mixing diminished, accounting for an increase in NO_x/NO_y and both NO_x and NO_y individually at the end of the day. Decomposition of PAN or other organic nitrates and continued deposition of NO_y may to a lesser extent contribute to the high NO_x/NO_y ratios observed in late afternoon. The mean NO_x/NO_y at Schefferville was nearly constant with time of day, reflecting the absence of local sources and uniform vertical profiles for NO_y and NO_y and the small deposition rate for NO_y at night.

Observations of the NO_x/NO_y ratio at Harvard Forest are similar to results from other mid-latitude forested sites [*Parrish et al.*, 1993; *Kleinman et al.*, 1994], where NO_x/NO_y reaches a minimum of ≈ 0.2 to 0.4 at midday in summer. The time of day when PAN/NO_y and HNO_3/NO_y were maximum at these sites coincided with the minimum in the NO_x/NO_y ratio. *Buhr et al.* [1990] noted a diurnal cycle with rapid PAN formation during the day at Scotia, Pennsylvania, and a decrease in PAN at night, which they attributed to thermal decomposition. *Shepson et al.* [1992] also observed rapid depletion of PAN from the surface layer during the night at a site in Ontario, Canada, but they argued that deposition of PAN must have been responsible because rates of thermal decomposition were too slow. We expect PAN to be an important component of NO_y at Harvard Forest as well. Although we observe significant rates of NO_y deposition at night (see section 4.3), we argue that diel pattern may be inconsistent with significant deposition of PAN.

The midday minimum in NO_x/NO_y (≈ 0.2) at Harvard Forest in summer appears to represent conditions throughout the mixed layer. The ratio was nearly identical for clean and polluted sectors, and only slightly higher than the ratio at Schefferville, even though ambient concentrations of NO_x and NO_y were smaller there by a factor of 10. These observations imply an important result: characteristic times for the cycle of NO_x oxidation and

Table 1. Summary Statistics of Midday (1000-1700) Concentrations for Selected Seasons and Surface-Wind Direction Sectors, 1900-1994

		Harvard Forest Summer			Harvard Forest Winter			Schefferville Summer1990
Species	Statistic	NW	E	SW	NW	E	SW	
NO_x, ppbv	*n*	360	147	287	344	123	182	180
	25%	0.46	0.74	0.62	1.22	3.00	2.01	0.027
	median	0.57	1.54	0.92	1.97	7.29	5.26	0.042
	mean	0.62	2.04	1.25	4.26	9.81	9.48	0.048
	s. d.	0.20	2.13	0.99	7.10	9.97	9.25	0.030
	75%	0.67	2.65	1.47	4.76	11.49	14.03	0.057
NO_y, ppbv	*n*	581	181	488	375	222	247	351
	25%	1.37	2.78	2.87	1.98	4.51	4.36	0.168
	median	1.87	4.36	4.73	3.36	7.64	10.98	0.237
	mean	2.33	4.67	5.05	5.69	10.17	13.29	0.308
	s. d.	1.41	2.26	2.69	6.34	7.83	10.18	0.249
	75%	2.80	6.16	6.83	6.87	14.13	20.39	0.371
O_3, ppbv	*n*	880	293	750	864	296	458	287
	25%	32.7	25.3	44.8	21.5	17.3	14.5	18.9
	median	39.2	34.0	55.7	28.5	24.6	22.2	22.6
	mean	40.3	36.5	57.7	27.1	23.2	21.5	23.8
	s. d.	12.0	15.0	18.9	10.8	11.2	12.0	7.3
	75%	44.8	45.6	68.6	34.4	31.3	30.3	27.9

decomposition of oxidized species to regenerate NO_x are short compared to the characteristic times for vertical and horizontal transport on regional scales.

The oxidized fraction of NO_y (1- NO_x/NO_y) [*Buhr et al.*, 1992]was lower in winter by factors of 2 and 4, respectively, for clean and polluted sectors, reflecting the decrease in rates for photochemical oxidation of NO_2 from summer to winter. However, this difference is much smaller than the 10-fold seasonal change in OH [*Spivakovsky* et al., 1990; *Goldstein et al.*, 1995] pointing to another important result: NO_x must be oxidized at significant rates by heterogeneous reactions [cf. *Li et al.*, 1993] as discussed further in section 4.3 and by M96.

4.2. Diel and Seasonal Patterns of Fluxes

On average, larger eddy fluxes and higher ambient concentrations of NO_y were associated with winds from the SW than with winds from the NW (Table 2) in both summer and winter, Fluxes of NO_y during winter were independent of time of day, as expected from the weak diel variation of NO_y concentrations and NO_x/NO_y ratio. During summer, however, the eddy fluxes of NO_y followed a strong diel cycle (Figure 9).

Mean deposition fluxes of NO_y at midday did not vary significantly with season (Table 2). This is a remarkable result providing strong indication of a primary role for heterogeneous oxidation of NO_x in winter. Moreover, even in summer the diel pattern of NO_y deposition indicates an appreciable contribution from heterogeneous oxidation of NO_x, primarily at night. Eddy fluxes of NO_y in summer increased sharply after sunrise to a maximum before noon, then declined during the afternoon to low nighttime values; peak NO_y fluxes preceded both the maximum in u* and the minimum in NO_x/NO_y. Because the contribution from PAN should peak in the afternoon [*Buhr et al.*, 1990; *Roberts et al.*, 1995] this pattern is inconsistent with significant deposition of PAN. Eddy fluxes of NO_y at Schefferville averaged ≈ 20% of the summertime values at Harvard Forest for winds from the clean sector. Deposition increased gradually over the morning to a peak

Table 2. Summary Statistics of Midday (1000-1700) Eddy Fluxes for Selected Seasons and Surface-Wind Direction Sectors, 1990-1994

		Harvard Forest Summer			Harvard Forest Winter			Schefferville Summer 1990
Species	Statistic	NW	E	SW	NW	E	SW	
NO_y Flux, μmole m^{-2} h^{-1}	*n*	485	162	440	249	129	177	351
	25%	-2.55	-3.58	-4.86	-3.03	-2.93	-4.94	-0.647
	median	-1.45	-2.16	-2.97	-1.44	-1.35	-2.64	-0.398
	mean	-2.24	-2.82	-4.19	-2.62	-2.40	-3.87	-0.525
	s. d.	2.80	2.72	4.98	3.38	3.20	4.05	0.445
	75%	-0.85	-1.20	-1.57	-0.71	-0.66	-1.21	-0.228
O_3 Flux, μmole m^{-2} h^{-1}	*n*	653	198	573	674	213	309	394
	25%	-53.3	-35.0	-66.2	-15.0	-8.0	-14.5	-8.3
	median	-39.9	-23.6	-45.6	-9.8	-4.8	-8.7	-10.8
	mean	-42.0	-27.1	-51.1	-11.0	-5.9	-11.2	-11.1
	s. d.	20.1	17.1	30.0	7.2	5.2	10.1	4.2
	75%	-28.2	-16.5	-30.1	-5.7	-2.7	-4.3	-13.5

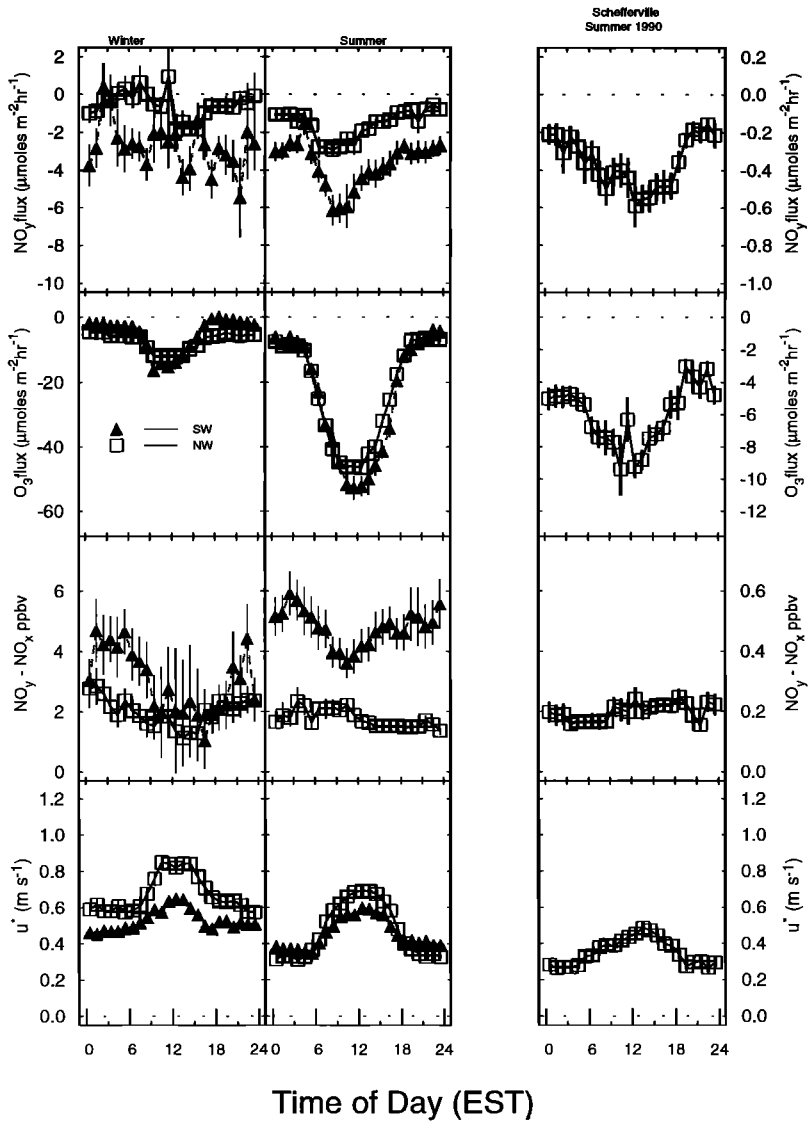

Figure 9. Mean diel cycles of NO_y and O_3 fluxes for winter (December - February) at Harvard Forest, column 1, and summer (June - August) at Harvard Forest, column 2, are shown for two dominant wind sectors: 270° - 45° is solid line and open square; 180° - 270° is long-dashed line and solid triangle. Vertical bars indicate the standard error about the mean. Very stable or unusually stormy periods are rejected by using only data for $0.1 < u^* < 1.5$ and $0.1 < u^* < 1$ m s^{-1} for winter and summer, respectively. Data for the period March 1990 - December 1994 are used. Mean diel cycles ± standard. error for Schefferville are shown for the same conditions of u^* ($0.1 < u^* < 1$ ms^{-1}) in column 3. Note the reduction in scale in the Schefferville plot.

at noon then declined over the afternoon to a minimum after sundown (Figure 9, column 3).

Eddy fluxes of O_3 during winter at Harvard Forest (Figure 9) had a distinct mid-day maximum, independent of wind sector, coincident with the peak in u*, reflecting efficient vertical transport. In summer, eddy fluxes of O_3 were identical for both clean and polluted wind sectors, despite the 50% difference in concentration (compare Tables 1 and 2). Peak fluxes, on average, occurred near or just before noon, coinciding with maximum PPFD. These results, especially the covariance with PPFD, appear consistent with significant influence of stomatal conductance on rates for O_3 uptake [*Baldocchi et al.*, 1987]. Fluxes of O_3 to the spruce woodland at Schefferville increased sharply after sunrise and reached a maximum before noon. The maximum mid-day O_3 flux at Schefferville was lower by a factor of 4 relative to Harvard Forest, though concentrations were only lower by about a factor of 2, reflecting reduced stomatal area, and hence lower deposition velocity at Schefferville (see next section).

4.3. Deposition Velocities

Comparison of deposition velocities for different chemical species ($V_{di} = -F_i/C_i$, where F_i and C_i denote flux and concentration of species i at a specified reference height) allows examination of factors affecting rates for dry deposition independent of ambient concentrations. Although there is evidence for slight NO_x uptake in the canopy during some periods, the contribution of NO_x to the NO_y deposition flux should be small because of the low NO_x concentrations (see section 4.4 below). Furthermore, the deposition velocity for total NO_y during well-mixed periods generally decreases as the fraction of NO_x increases (Figure 10). We therefore normalize the NO_y fluxes to $\{NO_y\text{-}NO_x\}$ to obtain a

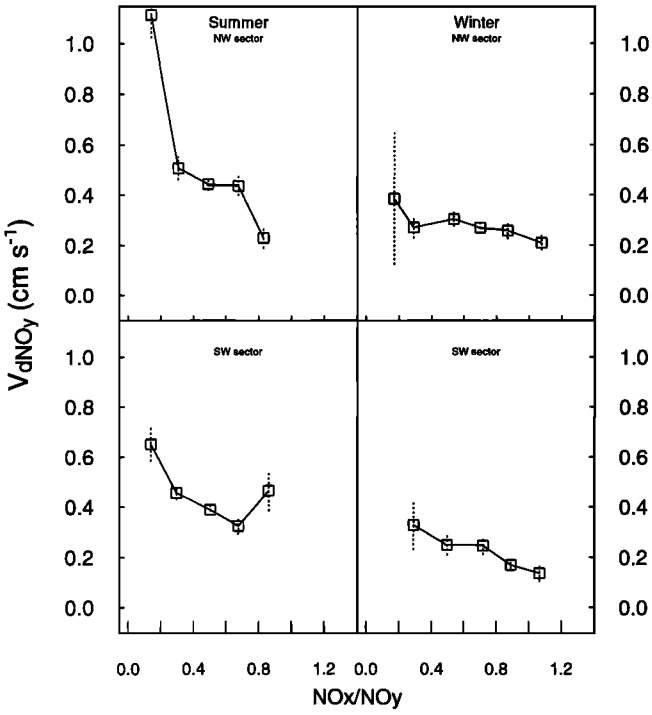

Figure 10. Mean NO_y deposition velocity is shown versus NO_x/NO_y for selected intervals of u* and wind sectors. Vertical segments represent the standard errors about the mean.

concentration-weighted average V_d for higher oxides of nitrogen, $V_{dNO_y-NO_x}$.

The diel pattern of deposition velocities for O_3 and {NO_y-NO_x} (Figure 11) mirrored the diel pattern for fluxes (Figure 9). Deposition velocities for {NO_y - NO_x}at Harvard Forest appear to be independent of wind direction, as we might have expected from the similar values of NO_x/NO_y. Deposition velocities at Schefferville were actually higher than at Harvard Forest, suggesting a greater proportion of HNO_3 relative to other species such as PAN due to differences in hydrocarbon concentrations and the older age of emissions that contribute to NO_y at this site. Variability in $V_{dNO_y-NO_x}$ during winter at Harvard Forest may be induced by rapid changes in concentrations through the canopy as pollution plumes pass the site as well as by measurement errors, at least in part, because the value of {NO_y - NO_x}/NO_y was often small. During the summer months, mean $V_{dNO_y-NO_x}$ peaked at 1.5 - 2 cm s^{-1} shortly after sunrise and dropped throughout the day to minimum value of ~ 0.5 cm s^{-1} at night. This unexpected pattern indicates that rapidly-depositing species are formed above the surface layer at night, providing a significant deposition flux during the early part of the day (see below).

During winter, O_3 deposition velocity had a weak diurnal cycle (Figure 11). The mid-day peak, ≈ 0.3 cm s^{-1}, presumably reflected diel changes in the rate of turbulent transport to the canopy (see Figure 12). The O_3 deposition velocities during summer peaked before 1200, consistent with measures of foliar activity that declined in the afternoon [*Amthor et al.*, 1994] (M. Goulden, unpublished data, 1995). There was a small difference between O_3 deposition velocities for winds from the clean and polluted sectors. The difference persists when we subdivide the data according to incident PPFD and friction velocity (see below).

To separate the influence of incident light and vertical mixing on surface deposition, we compute conditional medians of V_d for three light-level increments, segregated by wind sector, and plot against u* (Figure 12). Incident PPFD represents a surrogate for rates of photochemical reactions in all seasons and for rates of photosynthesis in summer. When leaves are present in the canopy

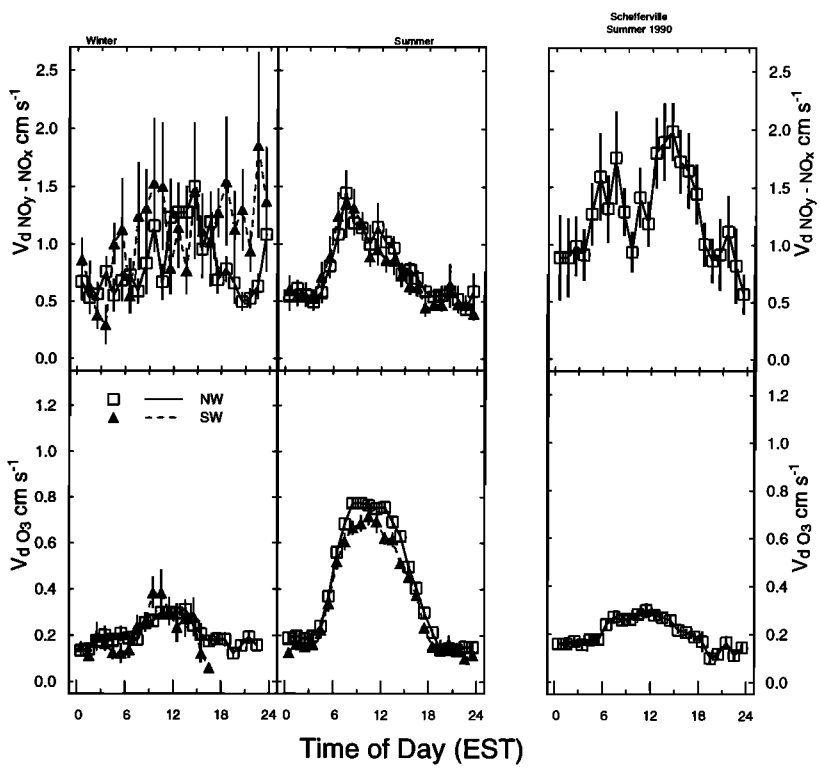

Figure 11. Mean deposition velocities computed for NO_y-NO_x and O_3 from winter and summer data at Harvard Forest and summer 1990 at Schefferville are shown against hour of the day. Data are conditionally averaged as for Figure 8. In addition, periods with O_3 < NO_y are excluded to avoid periods when O_3 chemical reactions may exceed O_3 deposition.

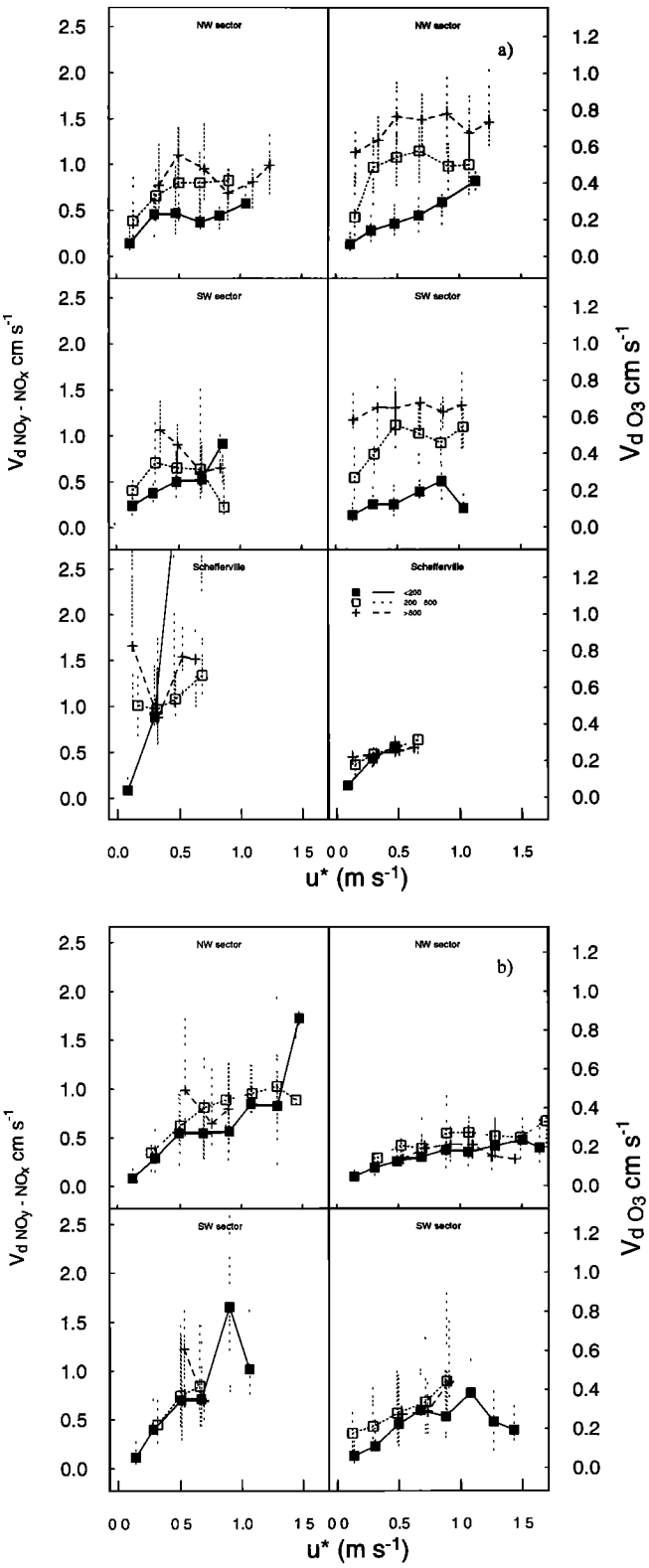

Figure 12. (a) Median deposition velocities for {NO_y - NO_x} and O_3 at Harvard Forest and Schefferville are shown as a function of u* for three ranges of photosynthetically-active photon flux density (PPFD). Solid symbols are low light, open squares are intermediate light, and pluses are high light. Maximum sunlight at midday in summer is ~ 1800 μmole m^{-2} s^{-1}. The left column is with clean-sector winds (270° - 45°); the right column is for polluted sector (180° - 270°) Vertical segments span the middle 50% of the data. (b) Same as Figure 12a for Harvard Forest in winter.

(Figure 12a), V_{dO_3} at Harvard Forest varies systematically with PPFD, consistent with stomatal control of O_3 uptake.

Deposition velocities for {NO_y - NO_x} in clean air (NW sector) increased, but only slightly, at photon fluxes > 200 μmole m^{-2} s^{-1}. Apparently, photochemical formation of readily depositable NO_y species is enhanced by a small amount as insolation increases, with photochemical formation of species, such as PAN, that do not readily deposit accounting for the weak or absent correlation between photon flux and NO_y deposition velocity. The vertical transport rate (friction velocity) appeared to limit $V_{dNO_y-NO_x}$ only at the lowest values of u*.

Deposition velocities during winter (when leaves are absent at Harvard Forest) for both {NO_y - NO_x} and O_3 were dependent on the vertical coupling (u*) and were largely independent of light levels (Figure 12b). The relationship between $V_{dNO_y-NO_x}$ and u* implies that the rate of vertical mixing is an important factor controlling NO_y deposition fluxes in winter, and the lack of dependence on sunlight implies that photochemistry is relatively unimportant then. The tendency for slightly higher $V_{dNO_y-NO_x}$ at comparable u* when winds were from SW, compared to the NW, could indicate that a larger fraction of NO_y - NO_x is composed of rapidly depositing species such as HNO_3 in the polluted (and generally warmer) air masses, even though the proportion of NO_x is higher.

Deposition of O_3 at Harvard Forest in winter is enhanced by increased vertical mixing, but canopy resistance still limits the mean O_3 deposition velocity to a maximum of ≈ 0.4 cm s^{-1}. The maximum V_d in winter is comparable to the maximum deposition under low light in summer. Deposition of O_3 to the bare canopy/snow surface exceeds the average V_d of 0.03 cm s^{-1} measured above bare snow [cf. *Wesely et al.*, 1981].

The role of canopy surface conductance in controlling O_3 fluxes can be assessed directly with data from Harvard Forest during the summer of 1993. Canopy surface conductance (g_c) was calculated from the water vapor flux, total energy input and momentum flux by inversion of the Penman-Monteith equation [*Shuttleworth et. al*, 1984]. Estimation of g_c from water flux is appropriate for Harvard Forest because subcanopy water fluxes, which include soil evaporation and transpiration by below-canopy vegetation, were small (10% in growing season) relative to water flux above the canopy [*Moore et al.*, 1996]. As expected, V_{dO_3} and g_c were highly correlated (r^2 = 0.61) (Figure 13). The slope was similar for all wind directions. The higher values of V_{dO_3} for winds from the NW sector, as compared to SW sector (Figure 11, 12), arises from differences in g_c, i.e., either from differences in the vegetation itself or response to higher pollution levels. The deposition velocity for {NO_y - NO_x}, however, was uncorrelated with g_c, consistent with the view that HNO_3 deposits readily to any surface [*Taylor et al.*, 1988].

Inferred role of heterogeneous oxidation of NO_x to HNO_3. The results imply that the diel pattern observed for $V_{dNO_y-NO_x}$ reflects diel changes in composition of {NO_y-NO_x} because fluxes of NO_y were not affected by stomatal conductance or by vertical mixing (except for very calm periods). *Trainer et al.* [1991] predicted that HNO_3 formed from NO_3 and N_2O_5 would be mixed to the surface at sunrise, when the nocturnal inversion layer is eroded, along with remnants of previous day's photochemical production. The present data appear to confirm this model. Heterogeneous production of HNO_3 may proceed in the surface layer as well [*Li et al.*, 1993], supporting part of the NO_y deposition flux at night, but efficient deposition prevents accumulation of HNO_3 near the ground. Note that the deposition velocity at Schefferville also had a morning peak corresponding to the

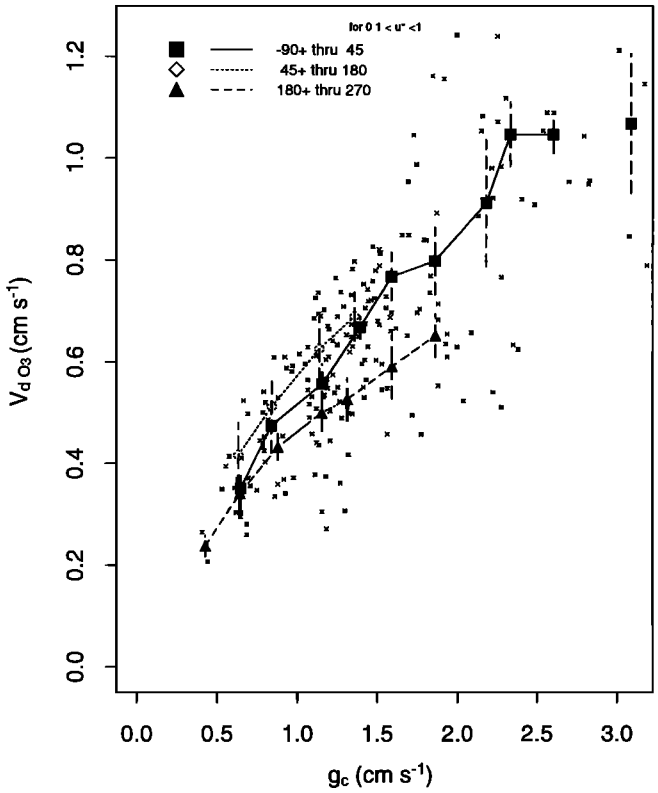

Figure 13. Ozone deposition velocity for the summer (June - August) of 1993 is shown versus the effective canopy stomatal conductance. Stomatal conductance was derived from measured H_2O, sensible heat and momentum fluxes. Lines and solid symbols indicate binned means; vertical dashed lines show the standard error.

breakdown of nocturnal inversion layer, likely for the same reason. (A late afternoon peak in $V_{dNO_y-NO_x}$ at Schefferville, observed later than the peak in NO_y flux is consistent with additional formation of HNO_3 from PAN decomposition coincident with maximum temperatures, OH concentrations, and vertical mixing [*Fan et al*, 1994].) Typical values of $V_{dNO_y-NO_x}$ are in the range 0.5 - 2 cm s^{-1} compared to reported values for HNO_3 deposition of 2-10 cm s^{-1} [*Hanson and Lindberg*, 1991]. These values are consistent with $HNO_3/(NO_y-NO_x)$ of 10-25% as is observed at Harvard Forest (B. Lefer and B. Talbot, unpublished data, 1995) and Schefferville [*Klemm et al.*, 1994], implying that HNO_3 is the dominant depositing species.

In the absence of significant changes in NO_y speciation, $V_{dNO_y-NO_x}$ should depend on aerodynamic and boundary layer resistances, R_a and R_b, which are functions of atmospheric turbulence [*Baldocchi et al.*, 1987; *Hicks et al.*, 1987]. Changes in NO_y speciation lead to changes in V_d. We may estimate the fraction of NO_y deposition flux that could be attributed to nocturnal production of HNO_3 by assuming a consistent relationship between $V_{dNO_y-NO_x}$ and $(R_a + R_b)$ ($V'_{dNO_y-NO_x} = V_d^0 + b/[R_a + R_b]$), as would be expected if there were no enhancement in the fraction of readily depositing NO_y species. We set V_d^0 to the minimum value for $V_{dNO_y-NO_x}$ at night, 0.25 cm s^{-1}, and derive b from midday values of V_d. The enhanced flux attributed to heterogeneous production of HNO_3 is in this model linearly related to the difference between observed $V_{dNO_y-NO_x}$ and $V'_{dNO_y-NO_x}$ in the morning; i.e., NO_y deposition fluxes are enhanced by 25% due to nocturnal formation of HNO_3 (Figure 14). If we assume that photochemically produced HNO_3 is depleted from the surface layer before midnight and that entrainment from aloft is negligible during night (i.e., $V_d^0 \leq 0.05$) then the deposition of NO_y after midnight may also be attributed to heterogeneous processes accounting for an additional 20% of the daily NO_y deposition.

We infer from the above analysis that roughly 45% of the dry deposition flux of NO_y is attributable to heterogeneous processes in summer. The rate of homogeneous oxidation of NO_x by OH in winter is only 10% of its summertime rate [*Goldstein et al.*, 1995; *Spivakovsky et al.*, 1990], yet midday deposition rates are similar; hence 90% of the NO_x oxidation in winter may be attributed to heterogenous processes.

4.4. Estimates of NO_x Flux From Vertical Profiles

The eddy covariance measurement determines the net flux for all species that emerge as NO from the gold catalyst. Deposition of NO_2 and emission of NO from soil contribute to the NO_y flux [*Stocker et al.*, 1993]. Our profile data for NO_x, in combination with eddy-covariance flux data, allow us to place limits on the magnitude of surface exchange fluxes for NO and NO_2 radicals.

Emissions of NO from soils. On average, concentrations of NO at Harvard Forest and Schefferville were slightly elevated near the forest floor during night, by 50 and 5 pptv, respectively,

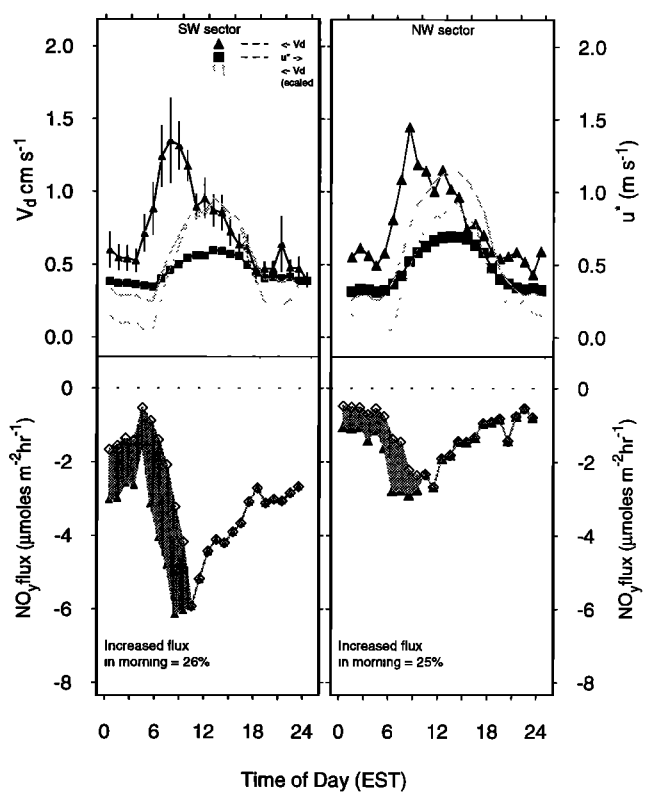

Figure 14. The observed diel course of V_d for $\{NO_y - NO_x\}$ (triangles) is compared to an assumed pattern (shaded lines) derived from the diel course of aerodynamic and boundary layer resistances $1/(R_a + R_b)$. R_a and R_b are estimated from friction velocity, u* (squares). The value of V_d after noon is assumed to represent the influence of photochemically produced HNO_3. The minimum value of V_d at night has been set here to 0.25 cm s^{-1}, roughly half the observed value, to reflect the depletion of HNO_3 when photochemical formation is shut down (top line); the bottom line is obtained by assuming V_d goes to 0.05 cm s^{-1} at night. In the bottom panels we scale the observed fluxes by ratio of observed and expected V_d to estimate the enhancement to NO_y deposition flux by nocturnal production of HNO_3 (shaded region).

implying some NO emission from soils. Because the reaction $NO + O_3 \rightarrow NO_2$ is very rapid compared to vertical mixing within the canopy (NO lifetime at 15° C with 30 ppbv of O_3 is 90 s), it would be misleading to evaluate NO gradients directly. Instead, the surface emission flux can be quantified from the mass balance equation for NO [*Parrish et al.*, 1987; *Kaplan et al.*, 1988], derived from equation (1) at night, when NO_2 is not photolyzed,

$$F_{NO} = \int_0^h k\,[O_3]\,[NO]\,dz + \frac{\partial}{\partial t}\int_0^h [NO]\,dz\,, \qquad (2)$$

where k is the second-order rate constant, t is time, z is height from the surface to the topmost sensor at z = h, and brackets denote concentration. Here F_{NO} represents a lower limit for emission at the surface if the flux of NO above z = h is not 0. Evaluation of equation (2) indicates weak emissions of NO from soils at Harvard Forest maximizing briefly in midsummer at about 0.9 μmole m^{-2} hr^{-1}, comparable to chamber measurements at other deciduous forest sites [*Williams et al.*, 1992]. Similar analysis of the Schefferville NO profiles implies even smaller soil NO emissions, 0 to 0.06 μmole m^{-2} hr^{-1}. In all cases, NO fluxes computed from equation (2) were much smaller than the observed net deposition of NO_y. The integrated O_3 loss from reaction with NO was <15% of the mean nighttime flux of O_3 measured above the canopy at Harvard Forest and <1% of the mean nighttime flux at Schefferville; reaction with soil-derived NO may be a minor contributor to nighttime O_3 deposition to the temperate deciduous forest during some seasons, but it is apparently unimportant in the spruce woodland.

NO_2 deposition. Chamber measurements indicate appreciable leaf conductances or deposition velocities for NO_2 uptake by vegetation, soils, and forest litter [*Hanson and Lindberg*, 1991; *Hanson et al.*, 1989]. However, some data suggest a compensation point at low concentrations, below which NO_2 deposition is negligible [*Johansson*, 1987; *Rondón et al.*, 1993; *Rondón and Granat*, 1994].

We examine the total NO_x rather than NO_2 profile data in order to avoid problems associated with shifts in NO/NO_2 partitioning due to gradients of irradiance and O_3 within the canopy [*Fitzjarrald and Lenschow*, 1983]. The observed NO_x profiles at Harvard Forest and Schefferville between the top sampling level and the surface (normalized to the concentration at the top) indicate an average net depletion of NO_x between the top level and the ground roughly half the mean O_3 depletion. We infer a deposition velocity for NO_2 <25% of the deposition velocity for $\{NO_y - NO_x\}$. Fluxes calculated from similarity with O_3 ($F_{NO_x} = F_{O_3}[\Delta O_3/\Delta NO_x]$) for unpolluted midday periods in summertime at Harvard Forest were -0.9 ± 3.6 μmole m^{-2} hr^{-1} (median = 0.5 μmole m^{-2} hr^{-1}) but not significantly different from 0 because individual measurements of ΔNO_x are distributed around zero with considerable scatter. A flux of this magnitude would account for only ≈ 25% of the NO_y deposition. Distortions in the NO_x profile from heterogeneity in soil NO emissions, inadequate resolution for the small differences in NO_x between measurement heights (< 100 pptv), and large, rapid fluctuations in NO_x concentrations at certain times of day preclude a more detailed quantification of NO_x deposition to the Harvard Forest and Schefferville canopies.

5. Conclusions

Results from a 5-year study of nitrogen oxide and ozone concentrations and fluxes at Harvard Forest in central Massachusetts, and during one summer at Schefferville in subarctic Quebec, demonstrated that long-term eddy-covariance flux measurements for NO_y are feasible. Eddy fluxes of NO_y to forest canopies were controlled by the rates of three environmental processes: horizontal transport from source regions, chemical reaction, and vertical mixing. In contrast to the observations for O_3 deposition, NO_y deposition fluxes were insensitive to changes in either leaf area or stomatal conductance. At both Harvard Forest and Schefferville the net NO_y flux was from the atmosphere to the canopy; soil emissions of NO were measurable but small. Heterogeneous formation of HNO_3, initiated by NO_2 reacting with O_3, was an effective pathway for NO_x removal.

The importance of advection from source regions was demonstrated by differences between wind sectors at Harvard Forest and by the contrast between the rural site at Harvard Forest and the remote site at Schefferville. Mean concentrations of NO_x and NO_y and deposition fluxes of NO_y were about twice as high at Harvard Forest during SW winds, which rapidly transport pollutants from major urban areas, than during periods of NW winds, which pass over fewer pollution source regions. Concentrations of NO_x and NO_y at Schefferville were a factor of 10 less and NO_y deposition fluxes were a factor of 5 less than the summertime mean values for clean sector winds at Harvard Forest.

Vertical transport is mediated by turbulence at the canopy interface, which is demonstrated by correlation between eddy fluxes and u*, as well as by boundary layer dynamics. Mean diel cycles, showing NO_x and NO_y concentration maxima at night for Harvard Forest, demonstrate trapping of emissions near the surface by the nocturnal inversion layer, with redistribution throughout the entire planetary boundary layer during the day. Away from pollution sources (as at Schefferville) similar mixed-layer dynamics produce an opposite pattern for surface concentrations, with midday maxima corresponding to deep mixing and minima at night when deposition depletes the surface layer beneath the nocturnal inversion. A more subtle effect of this diel variation of vertical mixing is the accumulation of readily-depositing species above the nocturnal inversion that are quickly mixed to the surface and removed after sunrise contributing to a rapid increase in concentrations, fluxes, and deposition velocities in early morning.

Seasonal changes in OH concentrations induce seasonal changes of ≈ 10x in NO_x oxidation rates due to homogeneous reactions. The similar rates of NO_y eddy fluxes in summer and winter and invariant background levels of NO_y imply, however, that the supply of HNO_3 or other depositable species does not decrease in proportion with OH concentrations. Evidently, heterogenous reactions must be important in winter. Even in summer, when OH concentrations reach seasonal maximum values, measurable NO_y fluxes during many nights, and the enhanced flux and V_d for $\{NO_y - NO_x\}$ shortly after sunrise, indicate that heterogenous oxidation of NO_x is an important process leading to removal of reactive nitrogen from the atmosphere.

Acknowledgments. This work was supported by grants from the National Aeronautics and Space Administration to Harvard University (NAG1-55, NAGW-3082) and to SUNY, Albany (NAG-11092), from the National Science Foundation to Harvard University (BSR-89-19300), from the U.S. Department of Energy to Harvard University and SUNY, Albany (Northeast Regional Center of the National Institute for Global Environmental Change, DOE Cooperative Agreement No. DE-FC03-90ER61010), by Harvard University (Harvard Forest and Division of Applied Sciences) and by the Alexander Host Foundation (fellowship to PSB). We thank the staffs of the McGill Subarctic Research Station at Schefferville, Harvard Forest, and the NASA Langley Research Center, for logistical support in the field. J. Demusz, N. Allen, T. Schiller, and E. Thompson provided electronics support for the data acquisition systems. We particularly thank A.

Colman, A. Hirsch, S. Roy, D. Sutton, and J. Sicker for their contributions to this project and D. Jacob for helpful discussions. The Harvard Forest data set is available by anonymous ftp at io.harvard.edu in the directory pub/nigec/HU_Wofsy/hf_data and the Web site http://www-as.harvard.edu.

References

Aber, J. D., K. J. Nadelhoffer, P. Steudler, and J. M. Melillo, Nitrogen saturation in northern forest ecosystems, *BioScience, 39*, 378-386, 1989.

Amthor, J.S., M. L. Goulden, J. W. Munger, and S. C.Wofsy, Testing a mechanistic model of forest-canopy mass and energy exchange using eddy-correlation: Carbon dioxide and ozone uptake by a mixed oak-maple stand, *Aust. J. Plant Phys., 21*, 623-651, 1994.

Bakwin, P. S., S. C. Wofsy, S.-M. Fan, and D. R. Fitzjarrald, Measurements of NO_x and NO_y concentrations and fluxes over Arctic tundra, *J. Geophys. Res., 97*, 16,545-16,557, 1992.

Bakwin, P. S., et al., Reactive nitrogen oxides and ozone above a taiga woodland, *J. Geophys. Res., 99*, 1927-1936, 1994.

Baldocchi, D. D., B. B. Hicks, and P. C. Camara, A canopy stomatal resistance model for gaseous deposition to vegetated surfaces, *Atmos. Environ., 21*, 91-101, 1987.

Bollinger, M. J., R. E. Sievers, D. W. Fahey, and F. C. Fehsenfeld, Conversion of nitrogen dioxide, nitric acid and n-propyl nitrate to nitric oxide by gold-catalyzed reduction with carbon monoxide, *Anal. Chem, 55*, 1980-1986, 1983.

Buhr, M. P., D. D. Parrish, R. B. Norton, F. C. Fehsenfeld, R. E. Seivers, and J. M. Roberts, Contribution of organic nitrates to the total reactive nitrogen budget at a rural eastern U.S. site, *J. Geophys. Res., 95*, 9809-9816, 1990.

Buhr, M. P., M. Trainer, D. D. Parrish, R. E. Sievers, and F. C. Fehsenfeld, Assessment of pollutant emission inventories by principal component analysis of ambient air measurements, *Geophys. Res. Lett., 19*, 1009-1012, 1992.

Carroll, M. A., and A. M. Thompson, Nitrogen oxides in the non-urban troposphere, in *Problems and Progress in Atmospheric Chemistry*, vol.. 3, *Advances in Physical Chemistry*, edited by J. R. Barker, World Sci., River Edge, N.J., 1995

Chameides, W. L., P. S. Kasibhatla, J. Yienger, H. Levy II., Growth of continental-scale metro-agro-plexes, regional ozone pollution, and world food production, *Science, 264*, 74-77, 1994.

Davidson, E. A., Fluxes of nitrous oxide and nitric oxide from terrestrial ecosystems, in *Microbial Production and Consumption of Greenhouse Gases: Methane, Nitrogen Oxides, and Halomethanes*, edited by. W. B. Whitman, pp. 219-235, Am. Soc. for Microbiol., Washington, D. C., 1991.

Davies, C. N., and M. Subari, Aspiration above wind velocity of aerosol with thin-walled nozzles facing and at right angles to the wind direction, *J. Aerosol Sci, 13*, 59-71, 1982.

Durka, W., E.-D. Schulze, G. Gebauer, and S. Voerkelius, Effects of forest decline on uptake and leaching of deposited nitrate determined from ^{15}N and ^{18}O measurements, *Nature, 372*, 765-767, 1994.

Environmental Protection Agency (EPA), The 1985 NAPAP emission inventory (version 2): Development of the annual data and modeler's tapes, *EPA Rep., EPA-600/7-89-012a*, Research Triangle Park, N. C., 1989.

Fahey, D. W., C. S. Eubank, G. Hubler, and F. C. Fehsenfeld, Evaluation of a catalytic reduction technique for the measurement of total reactive odd-nitrogen NO_y in the atmosphere, *J. Atmos. Chem., 3*, 435-468, 1986.

Fan, S.-M., S. C. Wofsy, P. S. Bakwin, D. J. Jacob, and D. R. Fitzjarrald, Atmosphere-biosphere exchange of CO_2 and O_3 in the central Amazon forest, *J. Geophys. Res., 95*, 16,851-16,864, 1990.

Fan, S.-M., S. C. Wofsy, P. S. Bakwin, D. J. Jacob, S. M. Anderson, P. L. Kebabian, J. B. McManus, C. E. Kolb, and D. R. Fitzjarrald, Micrometeorological measurements of CH_4 and CO_2 exchange between the atmosphere and the Subarctic tundra *J. Geophys. Res., 97*, 16,627-16,643, 1992.

Fan, S.-M., D. J. Jacob, D. L. Mauzerall, J. D. Bradshaw, S. T. Sandholm, D. R. Blake, H. B. Singh, R. W. Talbot, G. L. Gregory, and G. W. Sachse, Origin of tropospheric NO_x over Subarctic eastern Canada in summer, *J. Geophys. Res., 99*, 16,867-16,877, 1994.

Fazu, C., and P. Schwerdfeger, Flux-gradient relationships for momentum and heat over a rough natural surface, *Q. J. R. Meteorol. Soc., 115*, 335-352, 1989.

Fitzjarrald, D. R., and Lenschow, D. H., Mean concentration and flux profiles for chemically reactive species in the atmospheric surface layer, *Atmos. Environ., 17*, 2505-2512, 1983.

Fitzjarrald, D. R., and K. E. Moore, Growing season boundary layer climate and surface exchanges in the northern lichen woodland, *J. Geophys. Res., 99*, 1899-1917, 1994.

Gao, W., M. L. Wesely, and I. Y. Lee, A numerical study of the effects of air chemistry on fluxes of NO, NO_2, and O_3 near the surface, *J. Geophys. Res., 96*, 18,761-18,769, 1991.

Geigert, M. A., N. P. Nikolaidis, D. R. Miller, and J. Heitert, Deposition rates for sulfur and nitrogen to a hardwood forest in northern Connecticut, U. S. A., *Atmos. Environ., 28*, 1689-1697, 1994.

Goldstein, A. H., Non-methane hydrocarbons above a midlatitude forest: Biogenic emissions and seasonal concentration variations, Ph.D. thesis, Harvard Univ., Cambridge, Mass., 1994.

Goldstein, A. H., S. C. Wofsy, and C. M. Spivakovsky, Seasonal variations of non-methane hydrocarbons in rural New England: Constraints on OH concentrations in northern midlatitudes, *J. Geophys. Res., 100*, 21,023-21,033, 1995.

Goulden, M. L., J. W. Munger, S.-M. Fan, B. C. Daube, and S. C. Wofsy, Effects of interannual climate variability on the carbon dioxide exchange of a temperate deciduous forest, *Science*, in press, 1996a.

Goulden, M. L., J. W. Munger, S.-M. Fan, B.C. Daube, and S. C. Wofsy, Measurements of carbon storage by long-term eddy correlation: Methods and a critical evaluation of accuracy, *Global Change Biol.*, in press, 1996b.

Hanson, P. J., K. Rott, G. E. Taylor Jr., C. A. Gunderson, S. E. Lindberg, and B. M. Ross-Todd, NO_2 deposition to elements representative of a forest landscape, *Atmos. Environ., 23*, 1783-1794, 1989.

Hanson, P. J., and S. E. Lindberg, Dry deposition of reactive nitrogen compounds: A review of leaf, canopy and non-foliar measurements, *Atmos. Environ., 25A*, 1615-1634, 1991.

Hicks, B. B., D. D. Baldocchi, T. P. Meyers, R. P. Hosker, and D. R. Matt, A preliminary multiple resistance routine for deriving dry deposition velocities from measured quantities, *Water. Air Soil Pollut., 36*, 311-330, 1987.

Hicks, B. B., D. R. Matt, and R. T. McMillen, A micrometeorological investigation of surface exchange of O_3, SO_2 and NO_2: A case study, *Boundary Layer Meteorol., 47*, 321-336, 1989.

Holzworth, G. C., Mixing depths, wind speeds and air pollution potential for selected locations in the United States, *J. Appl. Meteorol., 6*, 1039-1044, 1967.

Houghton, J. T., et al., *Climate Change 1994, Radiative Forcing of Climate Change and an Evaluation of the IPCC IS92 Emission Scenarios*, 339 pp., Cambridge University Press, New York, 1995.

Huebert, B. J., and C. H. Robert, The Dry deposition of nitric acid to grass, *J. Geophys. Res., 90*, 2085-2090, 1985.

Johansson, C., Pine forest: A negligible sink for atmospheric NO_x in rural Sweden, *Tellus, 39B*, 426-438, 1987.

Johnson, D. W., and S. E. Lindberg, *Atmospheric Deposition and Forest Nutrient Cycling*, 707 pp., Springer-Verlag, New York, 1992.

Kaplan, W. A., S. C. Wofsy, M. Keller, and J. M. da Costa, Emission of NO and deposition of O_3 in a tropical forest system, *J. Geophys. Res., 93*, 1389-1395, 1988.

Kleinman, L., et al., Ozone formation at a rural site in the southeastern United States, *J. Geophys. Res., 99*, 3469-3482, 1994.

Klemm, O., R. W. Talbot, D. R. Fitzjarrald, K. I. Klemm, and B. L. Lefer, Low- to midtropospheric profiles and biosphere/troposphere fluxes of acidic gases in the summertime Canadian taiga, *J. Geophys. Res., 99*, 1687-1698, 1994.

Kley, D. and M. McFarland, Chemiluminescence detector for NO and NO_2, *Atmos. Technol., 12*, 63-69, 1980.

Kramm, G., and R. Dlugi, Modeling of the vertical fluxes of NO, NO_2, ozone, and HNO_3 in the atmospheric surface layer, *J. Atmos. Chem., 18*, 319-35, 1994.

Lenschow, D. H., and M. R. Raupach, The attenuation of fluctuations in scalar concentrations through sampling tubes, *J. Geophys. Res., 96*, 15,259-15,268, 1991.

Li, S.-M., K. G. Anlauf, and H. A. Wiebe, Heterogeneous nighttime production and deposition of particle nitrate at a rural site in North America during summer 1988, *J. Geophys Res., 98*, 5139-5157, 1993.

Liu, S. C., M. Trainer, F. C. Fehsenfeld, D.D. Parrish, E. J. Williams, D. W. Fahey, G. Hubler, and P. C. Murphy, Ozone production in the rural troposphere and the implications for regional and global ozone distributions, *J. Geophys. Res, 92*, 4191-4207, 1987.

Logan, J. A., Nitrogen oxides in the troposphere: Global and regional budgets, *J. Geophys. Res., 88*, 10,785-10,807, 1983.

Lovett, G. M., and S. E. Lindberg, Dry deposition of nitrate to a deciduous forest, *Biogeochemistry, 2*, 131-148, 1986.

Massman, W. J., The attenuation of concentration fluctuations in turbulent flow through a tube, *J. Geophys. Res., 96*, 15,269-15,273, 1991.

McMillen, R. T., An eddy correlation technique with extended applicability to non-simple terrain, *Boundary Layer Meteorol., 43*, 231-245, 1988.

Meyers, T. P., B. J. Huebert, and B. B. Hicks, HNO_3 deposition to a deciduous forest, *Boundary Layer Meteorol., 49*, 395-410, 1989.

Meyers, T. P., B. B. Hicks, R. P. Hosker Jr., J. D. Womack, and L. C.Satterfield, Dry deposition inferential measurement techniques, II, Seasonal and annual deposition rates of sulfur and nitrate, *Atmos. Environ., 25A*, 2361-2370, 1991.

Moore, K. E., D. R. Fitzjarrald, R. K. Sakai, M. L. Goulden, J. W. Munger, and S. C. Wofsy, Seasonal variation in radiative and turbulent exchange at a deciduous forest in central Massachusetts, *J. Appl. Meteorol. 35*, 122-134, 1996.

Müller, H., G. Kramm, F. Meixner, G. J. Dollard, D. Fowler, and M. Possanzini, Determination of HNO_3 dry deposition by modified Bowen ratio and aerodynamic profile techniques, *Tellus, 45B*, 346-367, 1993.

Padro, J., Seasonal contrasts in modelled and observed dry deposition velocities of O_3, SO_2, and NO_2 over three surfaces, *Atmos. Environ., 27A*, 807-814, 1993.

Parrish, D. D., E. J. Williams, D. W. Fahey, S. C. Liu, and F. C. Fehsenfeld, Measurement of nitrogen oxide fluxes from soils: Intercomparison of enclosure and gradient measurement techniques, *J. Geophys. Res. 92*, 2165-2173, 1987.

Parrish, D. D., et. al., The total reactive oxidized nitrogen levels and the partitioning between the individual species at six rural sites in eastern North America, *J. Geophys. Res., 98*, 2927-2939, 1993.

Ridley, B. A., M. A. Carroll, and G. L. Gregory, Measurements of nitric oxide in the boundary layer and free troposphere over the Pacific, *J. Geophys. Res., 92*, 2025-2047, 1987.

Ridley, B. A., M. A. Carroll, G. L. Gregory, and G. W. Sachse, NO and NO_2 in the troposphere: Technique and measurements in regions of a folded tropopause, *J. Geophys. Res., 93*, 15,813-15,830, 1988.

Raupach, M. R., R. A., Antonia, and S. Rajagopalan, Rough-wall turbulent boundary layers, *Appl. Mech. Rev. 44*, 1-25, 1991.

Roberts, J. M., et al., Relationships between PAN and ozone at sites in eastern North America, *J. Geophys. Res., 100*, 22,821-22,830, 1995.

Rondón, A., C. Johansson, and L. Granat, Dry deposition of nitrogen dioxide and ozone to coniferous forests, *J. Geophys. Res., 98*, 5159-5172, 1993.

Rondón, A., and L. Granat, Studies on the dry deposition of NO_2 to coniferous species at low NO_2 concentrations, *Tellus, 46*, 339-352, 1994.

Sandholm, S. J., et al., Summertime partitioning and budget of NO_y compounds in the troposphere over Alaska and Canada: ABLE 3B, *J. Geophys. Res., 99*, 1837-1861, 1994.

Schindler, D. W., and S. E. Bayley, The biosphere as an increasing sink for atmospheric carbon: Estimates from increased nitrogen deposition, *Global Biogeochem. Cycles, 7*, 717-733, 1993.

Schulze, E.-D., Air pollution and forest decline in a spruce *Picea abies* forest, *Science, 244*, 776-783, 1989.

Shepson, P. B., J. W. Bottenheim, E. R. Hastie, and A. Venkatram, Determination of the relative ozone and PAN deposition velocities at night, *Geophys. Res. Lett., 19*, 1121-1124, 1992.

Shuttleworth, J., et al., Eddy correlation measurements of energy partition for Amazonian forest, *Q. J. R. Meteorol. Soc., 110*, 1143-1162, 1984.

Singh, H. B., et al., Summertime distribution of PAN and other reactive nitrogen species in the northern high-latitude atmosphere of eastern Canada, *J. Geophys. Res., 99*, 1821-1835, 1994.

Spivakovsky C. M., R. Yevich, J. A. Logan, S. C. Wofsy, M. B. McElroy, and M. J. Prather, Tropospheric OH in a three-dimensional chemical tracer model: An assessment based on observations of CH_3CCl_3, *J. Geophys. Res., 95*, 18,433-18,440, 1990.

Stocker, D. W., D. H. Stedman, K. F. Zeller, W. J. Massman, and D. G. Fox, Fluxes of nitrogen oxides and ozone measured by eddy correlation over a shortgrass prairie, *J. Geophys. Res., 98*, 12,619-12,630, 1993.

Taylor, G. E. Jr., P. J. Hanson, and D. D. Baldocchi, Pollutant deposition to individual leaves and plant canopies: Site of regulation and relationship to injury, in *Assessment of Crop Loss From Air Pollutants*, edited by W. W. Heck, O. C. Taylor, and D. T. Tingey, pp. 227-257, Elsevier, New York, 1988.

Trainer, M., et.al., Observations and modeling of the reactive nitrogen photochemistry at a rural site, *J. Geophys. Res., 96*, 3045-3063, 1991.

Webb, E. K, G. I. Pearman, and R. Leuning, Correction of flux measurements for density effects due to heat and water vapour transfer, *Q. J. R. Meteorol. Soc., 106*, 85-100, 1980.

Wesely, M. L., D. R. Cook, and R. M. Williams, Field measurement of small ozone fluxes to snow, wet bare soil and lake water, *Boundary Layer Meteorol., 20*, 459-471, 1981.

Wesely, M. L., J. A. Eastman, D. H. Stedman, and E. D. Yalvac, An eddy-correlation measurement of NO_2 flux to vegetation and comparison to O_3 flux, *Atmos. Environ., 16*, 815-820, 1982.

Wesley, M. L., D. R. Cook, and R. L. Hart, Fluxes of gases and particles above a deciduous forest in wintertime, *Boundary Layer Meteorol., 27*, 237-255, 1983.

Williams, E. J., G. L. Hutchinson, and F. C. Fehsenfeld, NO_x and N_2O emissions from soil, *Global Biogeochem. Cycles, 6*, 351-388, 1992.

Wofsy, S. C., M. L. Goulden, J. W. Munger, S.-M. Fan, P. S. Bakwin, B. C. Daube, S. L. Bassow, and F. A. Bazzaz, Net exchange of CO_2 in a mid-latitude forest, *Science, 260*, 1314-1317, 1993.

B. C. Daube, M. L. Goulden, J. W. Munger (corresponding author), and S. C. Wofsy, Division of Applied Sciences and Department of Earth and Planetary Sciences, Harvard University, 401 ESL, 40 Oxford Street, Cambridge, MA 02138. (e-mail: jwm@io.harvard.edu)

D. R. Fitzjarrald and K. E. Moore, ASRC, SUNY-Albany, 100 Fuller Road, Albany, NY 12205.

P. S. Bakwin, Climate Monitoring and Diagnostics Laboratory, National Oceanic and Atmospheric Administration, Boulder, CO 80303.

S.-M. Fan, Atmospheric and Oceanic Sciences Program, Princeton University, Princeton, NJ 08540.

A. H. Goldstein, Environmental Science, Policy, and Management Department, University of California, Berkeley, 151 Hilgard Hall, Berkeley, CA 94720.

(Received June 29, 1995; revised January 3, 1996; accepted January 3, 1996.)